

DETERMINING HOW COMPOSITION CHANGES IN THE SEA SURFACE MICROLAYER
AFFECT CLOUD FORMATION

A Thesis

by

BRIANNA NICOLE HENDRICKSON

Submitted to the Office of Graduate and Professional Studies of
Texas A&M University
in partial fulfillment of the requirements for the degree of

MASTER OF SCIENCE

Chair of Committee,	Sarah D. Brooks
Committee Members,	Daniel C.O. Thornton
	Renyi Zhang
	Richard Moore
Head of Department,	Ramalingam Saravanan

December 2019

Major Subject: Atmospheric Sciences

Copyright 2019 Brianna Nicole Hendrickson

ABSTRACT

The potential influence of marine phytoplankton on cloud formation has been debated for more than forty years and remains unresolved due to uncertainty in the relative contribution of marine organic matter to cloud droplet formation. In this study, cloud condensation nuclei (CCN) measurements were conducted on aerosolized sea surface microlayer (SML) samples collected during the National Aeronautics and Space Administration (NASA) North Atlantic Aerosols and Marine Ecosystems Study (NAAMES) field campaigns. To determine the contribution of organics in marine sea spray to cloud formation, SML samples were desalinated to remove all salts. The CCN activity of the raw SML and desalinated samples were measured using a CCN counter (Droplet Measurement Technologies, Inc.). Sample composition was characterized using a wideband integrated bioaerosol sensor (WIBS), ion chromatography (IC), and a Shimadzu TOC-V. The analysis from the WIBS showed that aerosols produced from all SML samples and desalinated SML samples contained fluorescing material indicative of marine biological source matter. The CCN activity of SML samples was slightly reduced compared to pure salt and artificial seawater, as indicated by a mean hygroscopicity parameter, κ , of 0.96 ± 0.120 compared to a mean κ value of 1.34 ± 0.004 for NaCl and a mean κ value of 1.28 ± 0.004 for artificial seawater. Desalination of the SML samples decreased κ to a mean value of 0.36 ± 0.050 . To provide further insight on specific organic groups present in the samples, κ values were predicted based on the size and chemical composition of the aerosols. The chemical composition of the aerosols was assumed to be salts plus a specific organic compound. The organic concentration was determined assuming the total organic carbon (TOC) in the sample was entirely composed of that specific organic compound. Assuming seven different

representative organic components of marine aerosol including humic acid, fulvic acid, glucose, 6-glucose, Ribulose-1,5-bisphosphate carboxylase/oxygenase (RuBisCO), chlorophyll *a*, and triolein, the κ values of the samples were predicted and compared to the κ values from the CCN measurements. When the aerosol was treated as a mixture of salts and organics where the TOC was assumed to be entirely composed of RuBisCO, provided the closest predicted κ value to the measured κ value for the desalinated SML samples. The κ values predicted using an organic composition of RuBisCO for the desalinated SML samples ranged 0.44 ± 0.087 . Based on these results the best κ prediction for the raw SML samples would be a mixture of RuBisCO and NaCl. Varying the organic composition when predicting the κ values for the SML samples showed that the influence of the organics was insignificant compared to the influence from the salts on the κ values. The range of κ values across all the organic compositions considered for the SML samples was 1.28 ± 0.004 . This range of κ values matches the calculated κ values for artificial seawater, indicating that the salts present in artificial seawater largely influence the κ values for the SML samples. While the presence of organic material in the ocean surface waters may increase aerosol mass, cloud formation potential will be slightly weakened or unchanged compared to sea spray aerosol.

ACKNOWLEDGEMENTS

I would like to thank my committee chair, Dr. Brooks, and my committee members Dr. Thornton, Dr. Zhang, and Dr. Moore for their guidance and support throughout the course of this research.

I would also like to thank my family, friends, and fellow graduate students in the department for their encouragement and support.

CONTRIBUTORS AND FUNDING SOURCES

This work was supervised by a thesis committee consisting of Dr. Brooks and Dr. Zhang of the Department of Atmospheric Sciences at Texas A&M University, Dr. Thornton of the Department of Oceanography at Texas A&M University, and Dr. Moore of the NASA Langley Research Center. All work for the dissertation was completed independently by the student.

Measurements of the sea surface microlayer (SML) were conducted at the NASA Langley Research Center. These measurements included determining cloud condensation nuclei (CCN) activity, ion chromatography, and the wideband integrated bioaerosol sensor (WIBS). The desalination process of the SML samples was performed with the guidance of Dr. Thornton in the Department of Oceanography at Texas A&M University. The amino acid analysis was performed by the Carlson group at the University of California, Santa Barbara, Department of Ecology, Evolution, and Marine Biology, Santa Barbara, CA. The scanning electrical mobility sizer (SEMS) data was measured by the Russell group at Scripps Institute of Oceanography, University of California, San Diego, CA.

Funding for this project was provided by the NASA Earth Venture Suborbital-2 (EVS-2) Program (#NNX15AE68G).

NOMENCLATURE

CCN	Cloud Condensation Nuclei
CPC	Condensation Particle Counter
DOC	Dissolved Organic Carbon
DOM	Dissolved Organic Matter
DMA	Differential Mobility Analyzer
DSML	Desalinated Sea Surface Microlayer
GABA	Gamma-Aminobutyric Acid
HPLC	High Performance Liquid Chromatography
κ	Apparent hygroscopicity parameter
RuBisCO	Ribulose-1,5-bisphosphate carboxylase/oxygenase
SEMS	Scanning Electrical Mobility Sizer
SML	Sea Surface Microlayer
TDAA	Total Dissolved Amino Acids
TOC	Total Organic Carbon
WIBS	Wideband Integrated Bioaerosol Sensor
D	Critical dry particle diameter
S_c	Critical supersaturation
σ_{water}	Surface tension of pure water
$\sigma_{measured}$	Measured surface tension of samples
MW_{water}	Molecular weight of water
R	Universal gas constant

T	Absolute temperature
$MW_{solution}$	Molecular weight of solution
MW_{salts}	Molecular weight of salts in artificial seawater
ρ_{salts}	Density of salts in artificial seawater
ρ_{water}	Density of water
$\rho_{solution}$	Density of solution
MW_{org}	Molecular weight of organics
$n_{carbons}$	Number of carbons in organic molecule
W_i	Volume weighting factor for inorganics
W_o	Volume weighting factor for organics
W_i^{mole}	Molar weighting factor for inorganics
W_o^{mole}	Molar weighting factor for organics
$\rho_{particle}$	Density of the particle
ρ_{org}	Density of the organic
V	Volume of particle
i_{salts}	van't Hoff factor for salts in artificial seawater
i	van't Hoff factor
$mass_s$	Mass of solute
MW_s	Molecular weight of solute
i_{org}	van't Hoff factor for the organic
$mass_{mixture}$	Mass of inorganics and organics
$mass_{organic}$	Mass of organics

b	Parameter
c	Parameter
c_o	Parameter to calculate κ for organic composition only
c_m	Parameter to calculate κ for mixture of inorganics and organics
n_{salts}	Number of moles of salts in artificial seawater
n_{total}	Number of total moles
N	Number of carbon atoms in the organic molecule
SR	Saturation ratio
S_c	Critical saturation ratio
$A_{trapezoid}$	Area of a trapezoid
$base_1$	Base 1 of the trapezoid
$base_2$	Base 2 of the trapezoid
h	Height of the trapezoid

TABLE OF CONTENTS

	Page
ABSTRACT.....	ii
ACKNOWLEDGEMENTS.....	iv
CONTRIBUTORS AND FUNDING SOURCES	v
NOMENCLATURE	vi
TABLE OF CONTENTS.....	ix
LIST OF FIGURES	xi
LIST OF TABLES	xiii
1. INTRODUCTION	1
2. DATA AND METHODS	11
2.1. CCN Ship Measurements.....	11
2.2. Sample Collection and Storage.....	12
2.3. Desalination Process	13
2.4. NASA Langley Measurements	14
2.4.1. CCN Measurements of SML and DSML Samples	15
2.4.2. WIBS Measurements	16
2.4.3. Ion Chromatography Measurements.....	16
2.4.4. Surface Tension Measurements	16
2.5. Amino Acid Analysis.....	17
2.6. Scanning Electrical Mobility Sizer (SEMS) Data	17
3. κ CALCULATIONS.....	21
3.1. Calculating κ Values from CCN Measurements.....	23
3.2. κ Calculations Including Chemical Composition Data.....	25
3.2.1. Organics Selected for Calculations	25
3.2.2. Calculating κ Based on Chemical Composition Data.....	27
3.2.3. Calculating κ for Ambient Aerosol Data	34
3.2.4. Calculating κ for Ambient CCN Aerosol Including Composition Data	36
4. RESULTS	38

4.1. TOC	38
4.1.1. Amino Acid Analysis.....	38
4.2. Results from Measurements Made at NASA Langley Research Center	41
4.2.1. WIBS.....	41
4.2.2. Ion Chromatography	42
4.2.3. Surface Tension	43
4.2.4. CCN	45
4.2.5. Varying Organic Type in κ Calculation.....	49
4.3. Interpreting Ambient CCN Aerosol Cruise Data.....	54
4.3.1. Variation in κ and Critical Diameter by Station for Ambient CCN Aerosols	56
4.3.2. Ambient CCN Aerosol κ Results	58
5. DISCUSSION.....	61
6. CONCLUSION.....	64
REFERENCES	66
APPENDIX A.....	72
APPENDIX B	73
APPENDIX C	74
APPENDIX D.....	75
APPENDIX E	79
APPENDIX F.....	83
APPENDIX G.....	89

LIST OF FIGURES

	Page
Figure 1. NAAMES 3 cruise track (August-September 2017).....	11
Figure 2. NAAMES 4 cruise track (March-April 2018).....	12
Figure 3. Experimental setup from the NASA Langley Research Center	14
Figure 4. Nebulizer size distributions	15
Figure 5. SEMS size distribution	18
Figure 6. Example of CCN data used to determine critical diameter	19
Figure 7. Example of SEMS data used to determine critical diameter	20
Figure 8. Example of integrating under the SEMS data to find CCN critical diameter	20
Figure 9. Station averaged TOC concentration in SML samples	38
Figure 10. Total dissolved amino acids (TDAA) in SML samples and subsurface water samples	39
Figure 11. Beta-alanine and gamma-aminobutyric acid (GABA) in SML samples and subsurface water samples	40
Figure 12. Analysis of the aerosols generated by SML and DSML samples using the WIBS.....	41
Figure 13. Reduction in NaCl concentration in SML samples from portable refractometer and ion chromatography data	43
Figure 14. Surface tension measurements of SML and DSML samples	44
Figure 15. Critical diameter by station for aerosols generated by SML and DSML samples	46
Figure 16. κ by station for aerosols generated by SML and DSML samples	47
Figure 17. κ calculated from CCN measurements	48
Figure 18. κ calculated from CCN measurements and κ for reference salts.....	49
Figure 19. Measured and predicted κ values for SML samples.....	51
Figure 20. Measured and predicted κ values for DSML samples, assuming DSML samples contain no salts.	52

Figure 21. Varying the organic composition, assuming DSML samples contain salts using ion chromatography data	54
Figure 22. NAAMES 3 ambient CCN aerosol data	55
Figure 23. NAAMES 4 ambient CCN aerosol data	56
Figure 24. Critical diameters by station for ambient CCN aerosol measurements.....	57
Figure 25. κ by station for ambient CCN aerosol measurements	57
Figure 26. Varying composition data in ambient CCN aerosol κ measurements.....	59
Figure 27. Varying composition data in ambient CCN aerosol κ measurements displayed by station	59

LIST OF TABLES

	Page
Table 1. Samples selected from each field campaign to desalinate	13
Table 2. Properties of organic compounds	27

1. INTRODUCTION

The response of cloud characteristics to variations in aerosol concentration represents one of the largest uncertainties in understanding climate change today (Brooks & Thornton, 2018; Carslaw et al., 2013; IPCC, 2014). Due to the numerous processes that produce aerosols (natural, anthropogenic, primary, secondary), quantifying aerosol concentration and impacts on cloud formation are difficult. Specifically, in the category of naturally forming aerosols, marine aerosols are not well characterized. By definition marine aerosols are aerosols that are derived from oceanic sources. Marine aerosols produced through bubble bursting are primary aerosols and marine aerosols formed by chemical reactions in the atmosphere are secondary aerosols. The secondary aerosols can involve anthropogenic aerosols transported from continental sources. It is currently unknown how marine aerosols act as cloud condensation nuclei (CCN) or in what combination different types of aerosols are present in a marine environment. To better understand marine aerosols and their effects on the CCN population, it is necessary to sample marine aerosol populations and determine their ability to activate as CCN. It is currently assumed that the salts present in marine aerosols drive their ability to activate as CCN and the organics are assumed to have no significant influence on the cloud forming ability of the aerosol.

National Aeronautics and Space Administration (NASA) North Atlantic Aerosols and Marine Ecosystems Study (NAAMES) consisted of four month-long field campaigns focused on researching the effects of a phytoplankton bloom in the North Atlantic Ocean on aerosols and their ability to act as CCN (Behrenfeld et al., 2019). Each of the four campaigns was scheduled during a different period in the annual phytoplankton cycle. The mission of the NAAMES field

campaigns was to resolve key processes controlling ocean system functions, their influences on atmospheric aerosols and clouds, and their implications for climate. The campaigns were directed to answer how increasing surface ocean temperatures would affect the phytoplankton production, species compositions, and aerosol emissions. It is predicted by the Intergovernmental Panel on Climate Change (IPCC, 2014) that surface ocean temperatures will warm from +1.3°C to +2.8°C globally over the twenty-first century. Since oceans cover over 70% of the earth, natural events such as phytoplankton blooms that influence aerosol production could have a large impact on climate change. Currently how aerosols are affected by phytoplankton blooms and how this changes their ability to contribute to the CCN population are not well studied.

Several studies have been performed to mimic marine aerosols in a laboratory setting to better understand the influence of marine biological processes on aerosol production. In a laboratory study Moore et al. (2011) found that experiments with either sodium chloride or artificial seawater mixed with surfactants had only a 3% change in the CCN number concentrations over the remote boundary layer under simulated “bloom” conditions (M. J. K. Moore et al., 2011). These changes in CCN concentration from chemical changes due to the inclusion of marine organic matter during bubble bursting and sea spray aerosol formation had a limited effect on the climate. A study utilizing satellite and meteorological data over the Southern Ocean found that there was strong coupling between observed changes in marine biological productivity and microphysical properties of warm clouds located over a phytoplankton bloom (Meskhidze & Nenes, 2007). Unlike several other studies, Ovadnevaite et al. measured high concentrations of CCN during a time when the sea spray was enriched in organic matter. They suggested that this phenomenon was related to the enrichment of marine hydrogels in the sea spray aerosol

(Ovadnevaite et al., 2011). To better understand primary marine aerosols an in-situ particle generator (Sea Sweep) has been developed and used in various field campaigns (Bates et al., 2012). Sea Sweep generates bubbles 0.75 meters below the ocean surface through frits and then routes the aerosols to a suite of instrumentation onboard a ship. Due to the short time between the bubbles forming and the aerosols being sampled, there is a small chance of incorporating any aerosols formed through secondary processes. This ensures the capture and sampling of primary marine aerosols. In another study by Quinn et al., they reported field measurements that indicated that there was not a significant difference in CCN activity for high and low chlorophyll waters (Quinn et al., 2014). These results indicated that the organic carbon enrichment and CCN activity of nascent sea spray aerosol are relatively constant over different ocean regions. Modini et al. performed a tank study in which the amount of surfactant added to the tank was varied and bubble bursting was simulated in the tank (Modini, Russell, Deane, & Stokes, 2013). The size distribution of the particles produced by these bubbles had two or three separate aerosol modes. This indicated that there were multiple production mechanisms involved. The efficiency of particle production varied by more than one order of magnitude with changes in the solution film pressure. Since the film pressures used in this study could be reasonably achieved by sea slicks, the effect of the surfactant on the aerosol production is important to consider when predicting aerosol concentrations. In a series of field experiments by Russell et al. in the North Atlantic and Arctic they found the majority of organic mass in the clean regions was composed of carbohydrate-like compounds containing hydroxyl groups from primary ocean emissions (Russell, Hawkins, Frossard, Quinn, & Bates, 2010). These studies show how diverse the organics are in marine environments depending on the location, season, and meteorological conditions surrounding the sampling. Better quantifying the types of organics present in marine

cases will help improve the overall understanding of marine aerosols and how they activate as CCN.

Currently many of the published studies on marine aerosols include data from field campaigns located in coastal regions or the measurements were influenced by anthropogenic aerosol sources. Identifying the types of aerosols present and their origin can be a challenge for marine aerosol studies. Since these characteristics can affect the composition of the aerosols, this can affect the aerosols ability to activate as CCN. Even in a remote marine environment there can be influences from anthropogenic or land sources. A recent marine CCN study in the Caribbean Sea/tropical western North Atlantic measured mineral dust during almost the entire field campaign (Kristensen et al., 2016), these air masses were thought to have originated from Northern Africa (Gross et al., 2015). Since there was long-range transport of aerosols during this campaign, it is unknown if the organics measured in the gas and particle phases were also transported across the Atlantic Ocean. Identifying aerosol measurements sampled during times of clean marine air masses is difficult. Another study from the remote marine regions of the South China Sea/East Sea measured smoke from biomass burning, anthropogenic continental pollution, and emissions from shipping activities (Atwood et al., 2017). Hudson et al. found that 10% of emissions from ship exhaust were able to activate as CCN (Hudson et al., 2000). Taylor et al. measured marine air from the Atlantic Ocean that was predominantly sulfate based (Taylor et al., 2016). When the wind direction changed during sampling, the aerosol composition changed to contain ammonium nitrate and organics. This study demonstrates how quickly the composition of the aerosol can change which adds to the complexity of understanding the aerosol population and how the aerosol would activate as CCN. Kang et al. found that over the western North

Pacific both primary and secondary organic aerosols of terrestrial origin had a significant influence on marine aerosol chemistry from long-range atmospheric transport (Kang et al., 2018). A multi-decadal series of observations in Australia found that the marine biological source of reduced sulfur dominated CCN concentration in the summer but other components contributed to CCN over the full annual cycle (Gras & Keywood, 2017). In this study it is apparent that the composition of the aerosol varies seasonally. Seasonal and meteorological changes can impact the source and composition of the aerosol population. With changes in season, biological aerosols can vary depending on plant and tree pollen production. Seasonal impacts can also vary the amount of photochemistry occurring depending on the amount of sunlight present. Meteorological impacts can include the transport of anthropogenic or biological aerosols that can react with the local aerosol population. The NAAMES field campaigns provide data collected over the open ocean during times of clean marine air masses which can provide information about the biological processes occurring in the ocean and how these processes affect aerosol production.

One important topic of interest to connect the ocean processes with the aerosol populations is the sea surface microlayer (SML). The SML is the interface between the ocean and the atmosphere. The thickness of the SML is often debated since several different biological and meteorological processes must be taken into account to measure the thickness. The thickness of the SML is operationally defined as the uppermost 1-1,000 μm of the interface. The composition of the SML has been shown to be different from the composition of the subsurface waters. The SML enrichment of compounds has been attributed to surface-active matter collected by rising gas bubbles in the upper water column (Kuznetsova & Lee, 2002; Reinthaler, Sintes, & Herndl,

2008). The substances which are considered enriched in the SML are not currently agreed upon. Field measurements from the Pacific found that Coomassie Stainable Particles (CSP) was enriched in the SML when compared to the subsurface waters but that Transparent Exopolymer Particles (TEP) was not enriched in the SML (Thornton, 2018). CSP is a gel-like particle but less sticky than TEP. Phytoplankton and bacteria can release precursors for TEP and CSP which aggregate through abiotic processes. Another study found the TEP enrichment factor, determined by the ratio of the TEP concentration in the SML to the corresponding subsurface water, in the ocean to be 1.31 ± 0.52 (Wurl & Holmes, 2008). Similarly, Kuznetsova et al. (2005) found that TEP was enriched in microlayer and sea spray aerosol samples compared to bulk water (Kuznetsova, Lee, & Aller, 2005). Another study in the Pacific Ocean found enrichment in dissolved monosaccharides in the SML but not a significant enrichment of dissolved polysaccharides (Thornton, Brooks, & Chen, 2016). In measurements performed by Chen et al., they found that the carbohydrate species and amino acids were significantly enriched in the SML (Chen, Yang, Xia, & Wu, 2016). Samples analyzed in another study found enrichment in the SML of CSP and TEP (A. Engel & Galgani, 2016). A study by Zäncker et al. found the highest enrichment of organic matter in the open ocean (Zäncker, Bracher, Röttgers, & Engel, 2017). This was surprising due to the location having the lowest primary production and the highest wind speeds. The importance of the SML composition is related to the aerosols which form at the surface. Incorporation of the SML into marine aerosol particles can change their physical properties (Bigg and Leck (2008); Sellegri, O'Dowd, Yoon, Jennings, and de Leeuw (2006); (M. J. K. Moore et al., 2011)), affecting their ability to scatter light, take up water, and form clouds.

Despite the long-lasting interest in the physiochemical properties of the SML, studies on the microbial metabolism in the SML are still scarce, particularly for the open oceans comprising the vast majority of the oceans' surface (Reinthal et al., 2008). Laboratory studies have shown there can be significant differences in the molecular diversity within seawater that coincides with the evolution of a phytoplankton assemblage. Changes in molecular diversity in seawater affected aerosol's hygroscopicity (Cochran et al., 2017). Until recently the atmospheric community relied on chlorophyll-*a* concentration as a proxy for biological activity and emission of biogenic aerosol precursors; this is now being considered an oversimplification (Behrenfeld et al., 2019; Rinaldi et al., 2013). With the wide array of data available from the North Atlantic Aerosols and Marine Ecosystems Study (NAAMES) campaigns, other biological considerations can be included to link the observed atmospheric properties with the variations in ocean ecosystems.

It is well known that marine aerosols contain a large percentage of salts. Salt particles are considered hygroscopic due to their efficiency at taking up water. The hygroscopicity of a particle depends on the size and the composition of the particle. However, it is still not well understood how the organics present in marine aerosols affect their ability to act as CCN. With the concentration of marine aerosols being composed largely of salts, the influence of organics in these aerosols has not been well characterized. Understanding organic compound enrichment and microbial uptake and cycling in the SML requires improved knowledge of the chemical nature of organic molecules, the functioning of the ecosystem below and within the SML, and the mechanisms that transport organic matter into and out of the SML (Anja Engel et al., 2017).

Using samples from NAAMES, it is possible to better characterize the organics present in the SML and determine their effect on the aerosol population's ability to activate as CCN.

The NAAMES 3 (August-September 2017) and NAAMES 4 (March-April 2018) field campaigns included collecting SML samples to better characterize the ocean surface and try to correlate SML composition changes to changes seen in the aerosol populations concurrently. This study analyzes the SML samples collected during these campaigns and aerosolized the samples to test their ability to activate as CCN. A subset of the SML samples were desalinated. The desalinated sea surface microlayer (DSML) samples were aerosolized to determine their ability to activate as CCN. After the salts are removed from the samples, the ability to activate as CCN should be largely influenced by the organics remaining in the samples. This analysis will allow for a better characterization of how the organics present in a marine aerosol population affect cloud production. These results in conjunction with the other data from the WIBS and ion chromatography will provide more detailed insight into the composition of the SML.

When comparing different aerosol populations, it is common to calculate the apparent hygroscopicity parameter, κ , of each population. κ is a single variable to account for chemical effects on cloud activation (Petters & Kreidenweis, 2007). This allows field campaigns and laboratory experiments to report a single value that can be compared to results from other studies. Work by Collins et al. compared the κ values from various field campaigns and laboratory experiments. From these data the marine κ value ranged from 0.7 to 1.4 with an average of 0.95 ± 0.15 (Collins et al., 2016). Another study along the coast of Southern California found the hygroscopicity parameter to range from less than 0.1 to 1.4 with a campaign average of 0.22 ± 0.12 (Gaston et al., 2018). While these values seem lower than those reported by Collins et

al., they believed there may have been pollution or anthropogenic influences during the campaign. An aircraft study from Moore et al. over California calculated κ values from CCN measurements that varied from 0.10 to 0.25 (Moore et al., 2012). In a similar study over the Alaskan Arctic Moore et al. calculated κ values from CCN measurements that range from 0.1 to 0.3 (R. H. Moore et al., 2011). In a two-week study in remote marine regions of the South China Sea/East Sea, Atwood et al. found average κ values of 0.40 for samples dominated by aged accumulation mode smoke; 0.65 for accumulation mode marine aerosol; 0.60 in an anthropogenic aerosol plume; and 0.22 during a short period with elevated levels of volatile organic compounds (Atwood et al., 2017). From measurements made on the eastern coast of the United States there were two κ ranges identified, 0.20 ± 0.01 and 0.54 ± 0.03 (Phillips et al., 2018). According to a study by Pringle et al. the global mean κ for marine regions is 0.72 ± 0.24 (Pringle, Tost, Pozzer, Poschl, & Lelieveld, 2010). While some of these κ values between studies are similar, there is a wide range of reported marine κ values. Some of this is due to variations in sampling methods and locations. The influence of anthropogenic sources will decrease the κ value from a purely marine case. There can also be seasonal changes or meteorological parameters that vary between studies.

Once the most representative organic composition for the SML and DSML samples has been determined, this composition can be used to predict the κ values for the ambient CCN aerosol population. Since the SML is the interface between the ocean and the atmosphere, particles originating from the SML can be lofted into the atmosphere. Therefore, the composition of the SML will affect the aerosols ability to activate as CCN. Measurements of ambient aerosol in the marine boundary layer have suggested a relationship between the biological activity in the

ocean's surface and the organic mass fraction of marine aerosol (Collins et al., 2016; O'Dowd et al., 2004). Knowing additional information about the organic composition in the SML could provide additional information about the organics present in the ambient CCN aerosol population. Will the most representative organic composition for the SML also be the most representative organic composition for the ambient CCN aerosols measured? Comparing the predicted κ values for the SML samples and the ambient aerosol measurements using chemical composition data could show that the aerosols generated by the SML are being lofted into the atmosphere and are being measured by the ambient aerosols.

2. DATA AND METHODS

2.1. CCN Ship Measurements

During NAAMES 3 and NAAMES 4, aerosol measurements were made on the ship using a condensation particle counter (CPC), a differential mobility analyzer (DMA), and a CCN counter. The CPC measured the total number of aerosols and the CCN counter measured the number of aerosols able to activate as CCN at a specific supersaturation. The aerosols being measured were sized by the DMA to provide the number of particles able to activate at a specific supersaturation and diameter. From these data the κ values of the ambient CCN aerosols was calculated. The total concentration of the aerosols and the activation of the aerosols as CCN varied between NAAMES 3 and NAAMES 4. Figure 1 and Figure 2 show the paths taken by the ship during the NAAMES 3 and NAAMES 4 campaigns respectively.

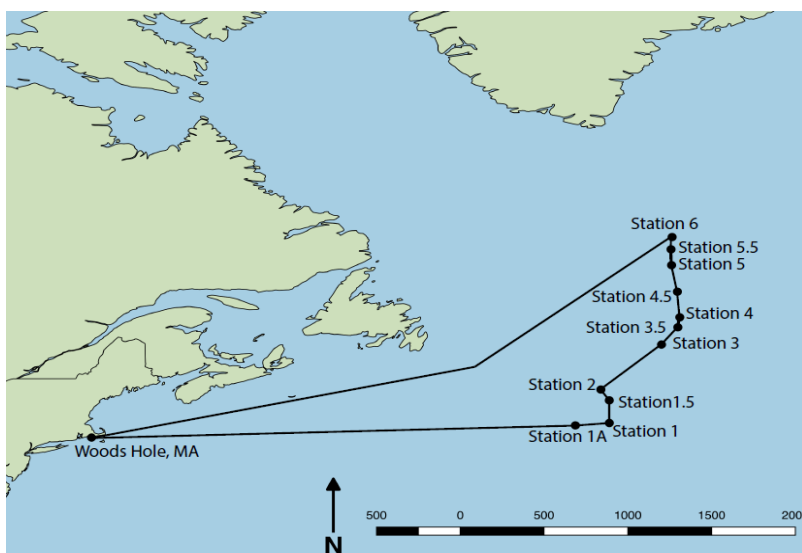


Figure 1. NAAMES 3 cruise track (August-September 2017)

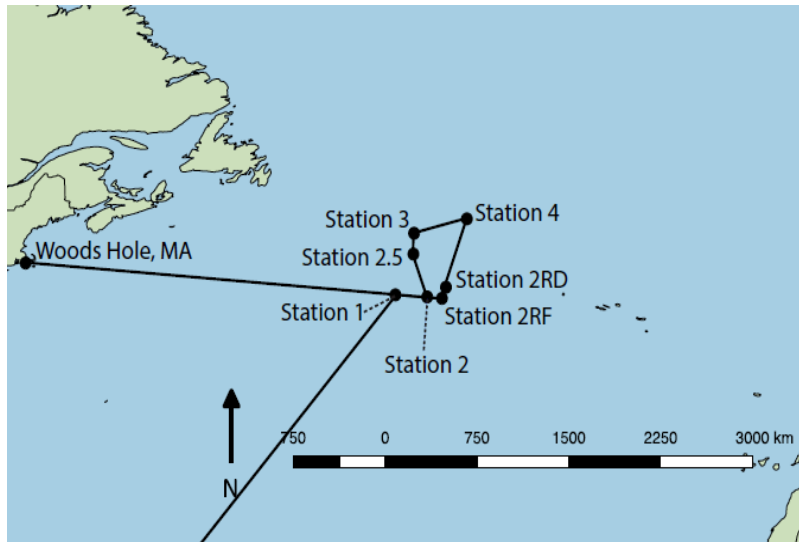


Figure 2. NAAMES 4 cruise track (March-April 2018)

2.2. Sample Collection and Storage

SML samples from the NAAMES 3 and NAAMES 4 field campaigns were collected using a Garrett screen (Garrett, 1965). To sample the SML a Garrett screen was attached to a rope and lowered over the right side of the *R.V. Atlantis*. The screen was lowered until it lightly touched the surface of the ocean and then it was pulled back up to the deck. The Garrett screen was held at an angle to allow the microlayer sample to run off the screen into a glass funnel and then into a container for collection. Depending on the amount of sample required by each group for analysis, the screen was lowered numerous times until the volume needed was collected. When handling the Garrett screen, funnel, and container gloves were worn to prevent any contamination. To clean the screen, funnel, and container between sampling periods Milli-Q water was used. To avoid contaminating the equipment, no additional cleaning products or soaps were used for cleaning. The same procedure and equipment were used for both field campaigns that sampled the SML. Samples were placed immediately into a -80°C freezer to preserve the samples until

they could be analyzed. The samples were stored in bottles that had been acid treated and rinsed before being used to store samples.

2.3. Desalination Process

A subset of four samples were selected for desalination, these samples are shown in Table 1. These samples allowed for the comparison of SML samples containing salts to SML samples that had the salts removed. Two samples were chosen from each field campaign, at the station with the lowest chlorophyll *a* concentration and at the station with the highest chlorophyll *a* concentration. To begin the desalination process, the samples were removed from the -80°C freezer and allowed to thaw at room temperature. After the samples had thawed, the salinity of each sample was determined using a portable refractometer. 10 ml of each sample was removed from the bottles and placed inside dialysis tubing. The dialysis tubing had a pore size of 1,000 Daltons. The details of the dialysis tubing and the steps for desalinating the samples can be found in Appendix A.

Table 1. Samples selected from each field campaign to desalinate

Sample	Chlorophyll <i>a</i> Concentration (mg/m³)	Initial Salinity** (ppt)	Final Salinity** (ppt)
NAAMES 3 Station 1	Lowest, 0.05	40	~0
NAAMES 3 Station 6	Highest, 0.68	36	~0
NAAMES 4 Station 2	Highest, 0.84	39	~0
NAAMES 4 Station 4	Lowest*, 0.39	38	~0

*the lowest chlorophyll *a* station did not have a microlayer sample, this represents the second lowest chlorophyll *a* sample from NAAMES 4

**the limit of detection for the portable refractometer was 1.7 ppt

2.4. NASA Langley Measurements

The SML samples and DSML samples were taken to the NASA Langley Research Center for further analysis. This analysis included measurements from the wideband integrated bioaerosol sensor (WIBS), ion chromatography (IC), and cloud condensation nuclei counter (CCN counter).

The setup used at the NASA Langley Research Center is shown in Figure 3.

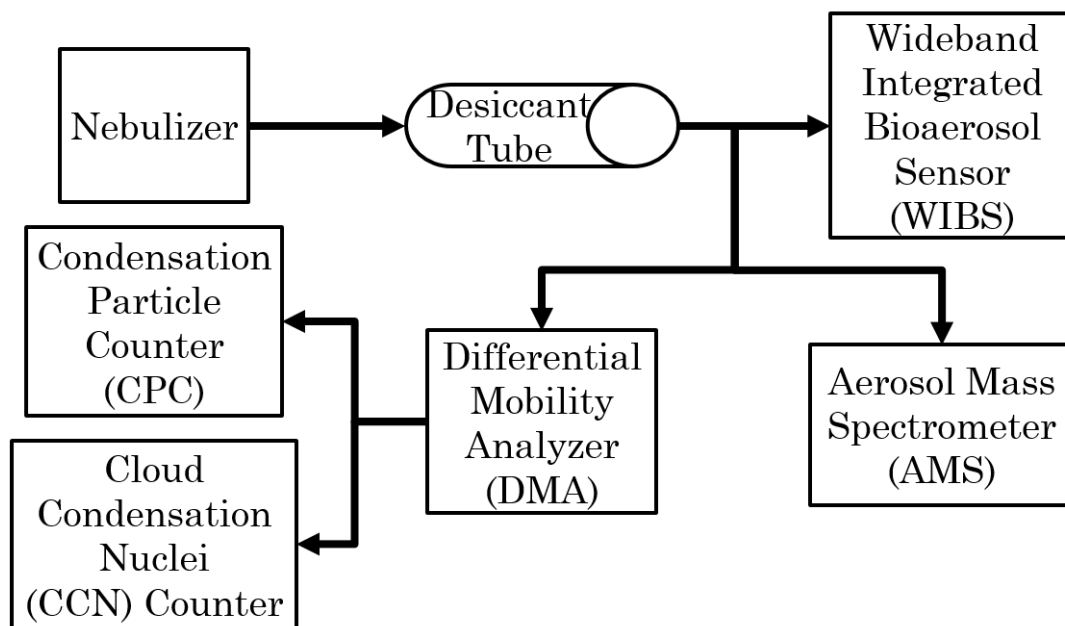


Figure 3. Experimental setup from the NASA Langley Research Center

The aerosols generated by the nebulizer were single mode with similar size distributions generated by each of the SML samples as shown in Figure 4.

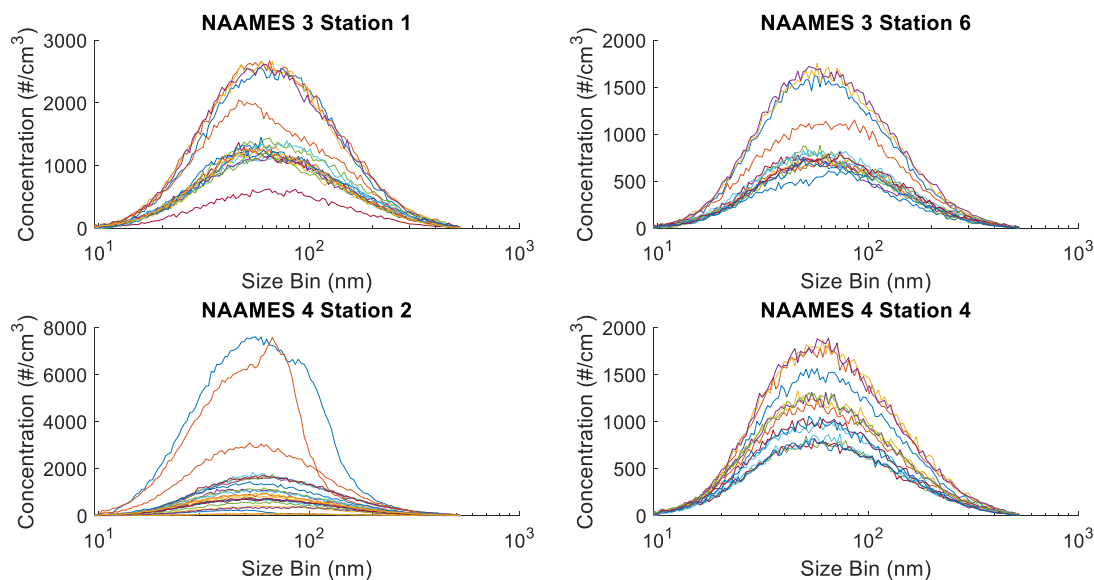


Figure 4. Nebulizer size distributions

Size distributions measured from aerosolizing the SML samples. Multiple lines represent different scans of the size distribution for each SML sample. The size bins describe the diameters of aerosols being measured.

2.4.1. CCN Measurements of SML and DSML Samples

SML and DSML samples were analyzed using a CCN counter to measure the aerosols ability to activate as CCN. The same procedure was used for the DSML samples. A scan of the size of the particles able to activate under each supersaturation selected by the CCN counter was measured. In order to predict κ values using chemical composition data the particle size of the SML and DSML aerosols are needed. The concentration of aerosols able to activate as CCN was also measured at each supersaturation. The aerosol size and abundance able to activate as CCN could be compared between the SML and DSML samples. These results showed how large the influence of salt was to the CCN activity and also helped to better quantify the effects of organics on the CCN activity.

2.4.2. WIBS Measurements

To determine if the SML and DSML samples contained biological material a wideband integrated bioaerosol sensor (WIBS) was used. The WIBS uses a UV xenon source to excite fluorescence in individual particles. The UV lamp causes the aerosols to fluoresce at specific wavelengths that are different from the excitation wavelengths. These wavelengths are chosen to optimize the detection of common bioaerosol components of tryptophan and nicotinamide adenine dinucleotide (NADH). The SML and DSML samples were aerosolized and then measured using the WIBS to determine if fluorescence of the particles could be measured.

2.4.3. Ion Chromatography Measurements

To provide measurements of the inorganics before and after the desalination process, ion chromatography was used in addition to the portable refractometer. These data provided an indicator of how efficient the desalination process was at removing the salts from the SML samples. The ion chromatography is also more precise than the portable refractometer.

2.4.4. Surface Tension Measurements

The surface tension was measured for each SML and DSML sample using a pendant drop tensiometer. When determining a κ value the surface tension of the water was needed as an input. Commonly the surface tension is assumed to be that of pure water. In marine cases this is often a poor assumption because it could lead to inaccuracy in predicting CCN. Surface active microgels will reduce surface tension and allow CCN to activate at lower supersaturations (Brooks & Thornton, 2018; Moore, Ingall, Sorooshian, & Nenes, 2008). For this reason, the measured surface tension of the SML and DSML samples was used in the calculations for κ .

2.5. Amino Acid Analysis

The amino acid analysis was performed by the Carlson group at the University of California, Santa Barbara, Department of Ecology, Evolution, and Marine Biology, Santa Barbara, CA. Using the SML samples to perform an amino acid analysis identifies the peaks of eighteen biologically significant dissolved amino acids through high performance liquid chromatography (HPLC). The eighteen dissolved amino acids are aspartic acid, glutamic acid, histidine, serine, arginine, threonine, glycine, tau protein, β -alanine, tyrosine, alanine, γ -aminobutyric acid, methionine, valine, phenylalanine, isoleucine, leucine, and lysine. From this analysis the concentrations of a specific amino acid relative to the total of the dissolved amino acids (and percentage) in units of nM amino acid or after conversions nM C are measured. These data were used to relate the HPLC output to the bulk dissolved organic carbon measurements to better quantify the percentage of total dissolved amino acids relative to the dissolved organic carbon. The amino acid analysis can provide information about the age of the dissolved organic material (DOM). Knowing additional information about the DOM age can provide insight into the size of the organic molecules present in the SML samples.

2.6. Scanning Electrical Mobility Sizer (SEMS) Data

The scanning electrical mobility sizer (SEMS) data was measured by the Russell group at Scripps Institute of Oceanography, University of California, San Diego, CA. The SEMS data provided the size distribution of ambient aerosols measured throughout the cruises. Figure 5 shows the size distributions measured during the microlayer sampling for each of the four samples used in this study. When comparing the size distribution from the SEMS to the size distribution of the nebulizer it is clear that the SEMS had more variability in the data. Some of

the SEMS size distributions have multiple modes in the aerosol data. The SEMS data also had aerosol concentrations being measured at much larger sizes than the nebulizer.

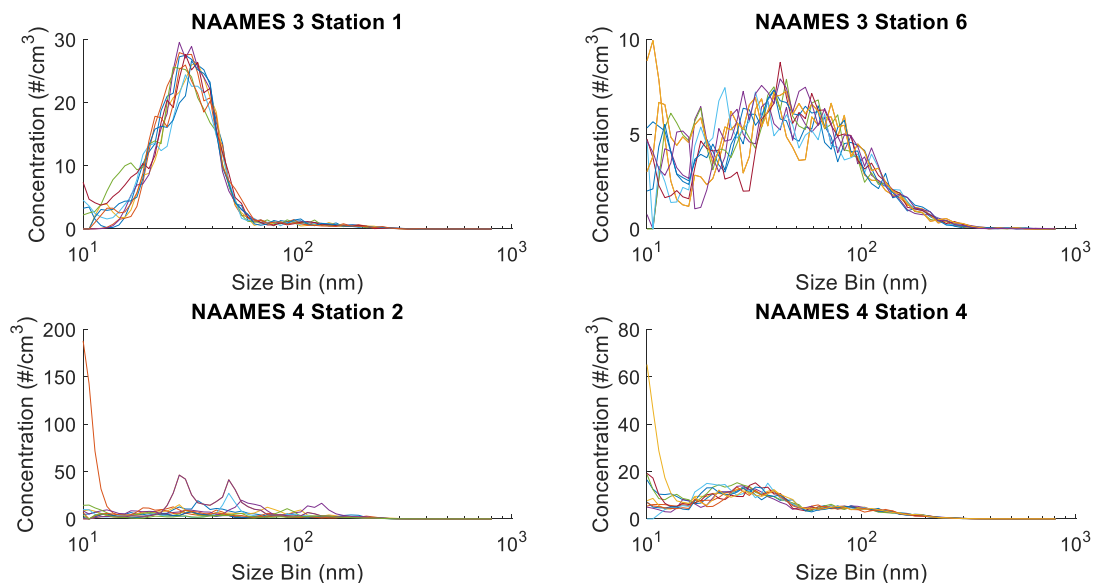


Figure 5. SEMS size distribution

Size distributions measured during times when the SML was being sampled. The multiple lines shows the individual size distributions measured during the sampling. The size bins describe the diameters of aerosols being measured.

Since the ambient CCN aerosol data measured on the ship did not have an associated size, the SEMS data was used to calculate the aerosol size. With the concentration of particles able to activate as CCN at a specific time and supersaturation, the same time was identified in the SEMS data. By integrating under the SEMS data beginning from the largest size bin and integrating toward smaller size bins, the total concentration of particles in a size range was calculated. Making the assumption that all particles larger than the critical diameter will activate as CCN, then the critical diameter of the aerosol population is the lower bound of integration where the number of particles measured by integrating under the SEMS data is equal to the concentration of particles able to activate as CCN. The ambient aerosol size is needed to calculate the κ value.

This allows the κ values from the ambient CCN aerosol data to be compared to the κ values from aerosols generated by the SML and DSML samples. To further explain this process, the figures below demonstrate how the CCN data and the SEMS data can be used to determine a critical diameter. During the time that the microlayer samples were being collected the CCN instrument was able to measure CCN concentrations at each set supersaturation once. Figure 6 is showing the last sixty seconds of data measured by the CCN instrument as a specific supersaturation. This provides an average CCN concentration at that supersaturation. Then the same time the CCN data was collected was identified in the SEMS data, this is shown in Figure 7. By integrating under the SEMS data from the largest size bins until the concentration is equal to the CCN concentration provide the critical diameter. This process is shown in Figure 8.

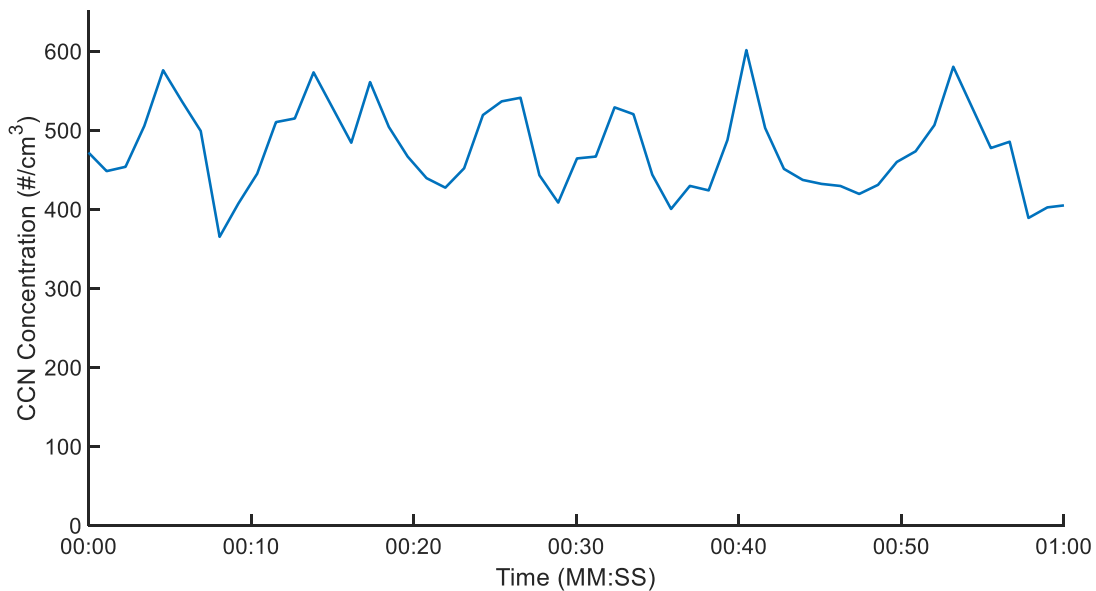


Figure 6. Example of CCN data used to determine critical diameter

This is the last sixty seconds of CCN data measured during a specific supersaturation while the microlayer samples were being collected.

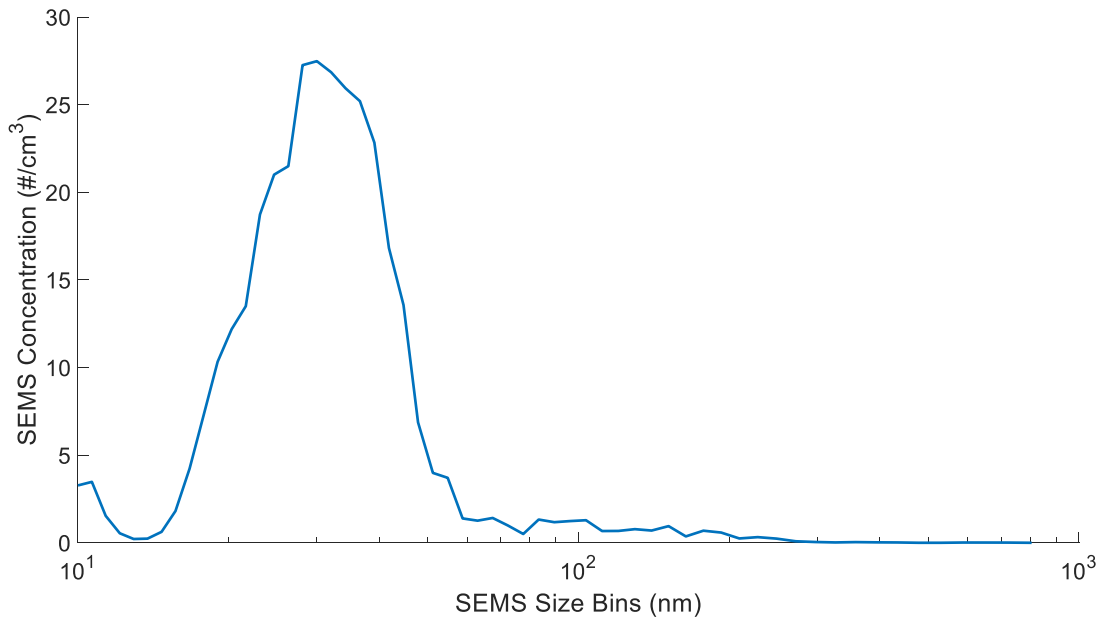


Figure 7. Example of SEMS data used to determine critical diameter

This is the SEMS size distribution data measured while the CCN data shown in Figure 6 was being collected.

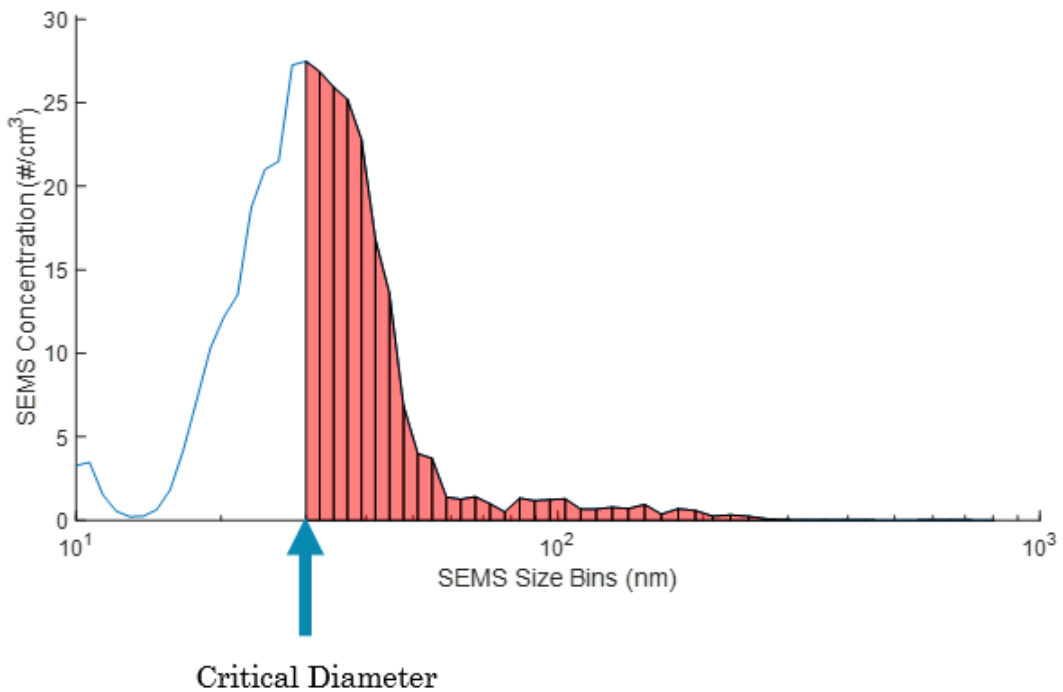


Figure 8. Example of integrating under the SEMS data to find CCN critical diameter

Using the average CCN concentration from Figure 6, the data under the SEMS curve was integrated until the concentration was equal to the CCN concentration. This point identified the critical diameter.

3. κ CALCULATIONS

Köhler theory describes an aerosol's ability to activate as a CCN and form cloud droplets (Köhler, 1936). This is dependent upon the aerosol's physical and chemical properties. Petters and Kreidenweis reformulated the Köhler equation as κ -Köhler theory (Petters & Kreidenweis, 2007). κ -Köhler theory calculates a κ value for an aerosol. κ is the hygroscopicity parameter and a single variable to account for chemical effects on cloud activation. The CCN measured κ values are calculated for each size of the aerosol and each supersaturation of the CCN instrument. In order to see the effects of different chemical compositions on the κ values, a κ value can be predicted using Köhler Theory and measured chemical composition. The two different κ values (one from CCN measurements and one from predictions to include chemical composition data) can then be compared to see how accurate the composition inputs were when predicting the κ values. To calculate κ from the CCN measurements the critical diameter and the critical supersaturation are needed. Both of these values can be determined using measurements from the CCN instrument. Then these values can be used to calculate a κ value, in this κ calculation there is not any information being provided about the chemical composition of the aerosol.

To predict a κ value for the CCN measurements that includes chemical composition data, the chemical composition inputs are the concentration of salts and the concentration of organics. The concentration of salts present before desalination was determined using the salinity of the samples measured by the portable refractometer and assumed to have the composition of artificial seawater. The concentration of salts present after the desalination process was

determined using ion chromatography data and portable refractometer data. The ion chromatography data showed that the concentration of NaCl in the microlayer samples decreased by 99.95% from the desalination process. The amount of salts remaining after desalination was assumed to be 0.05% of the salts present in the raw microlayer samples assuming the composition of artificial seawater. For the artificial seawater composition, the salts considered were sodium chloride, sodium sulfate, and magnesium sulfate. The concentration of organics was determined using the total organic carbon (TOC) data. The TOC concentration was converted from $\frac{\mu\text{moles C}}{L}$ to $\frac{g}{L}$ based on the representative organic compounds of the microlayer. The SML predicted κ values were calculated assuming the amount of salts (from salinity measurements) and organics (from TOC measurements) as the chemical composition inputs. For the predicted κ values for the DSML samples, the organic inputs were the same as the SML predicted κ values, but the salt concentration used was determined by applying the reduction in NaCl from the ion chromatography data to the concentration of salts in artificial seawater. In order to look at these different ratios of organics to inorganics (in SML and DSML samples), weighting factors were determined for the inorganics and the organics. These weighting factors were calculated following the work outlined by Petters et al. 2013 (Petters & Kreidenweis, 2013) and were applied to the density, the molecular weight, and the van't Hoff factor for the particle.

To calculate κ from ambient CCN measurements the diameter of the particle and the supersaturation are needed. Since the ambient CCN aerosol data measured on the ship did not have an associated size, the SEMS data was used to calculate the aerosol size. With the concentration of particles able to activate as CCN at a specific time and supersaturation, the same time was identified in the SEMS data. By integrating under the SEMS data beginning from the

largest size bin and integrating toward smaller size bins, the total concentration of particles in a size range was calculated. Making the assumption that all particles larger than the critical diameter will activate as CCN, then the critical diameter of the aerosol population is the lower bound of integration where the number of particles measured by the SEMS is equal to the concentration of particles able to activate as CCN. Once this critical diameter has been determined the supersaturation set within the CCN during this time was considered the critical supersaturation. Using these values, the κ value can be calculated for the ambient CCN aerosol.

To predict a κ value from ambient CCN measurements and chemical composition data assumptions must be made about the amount of organics and inorganics present in the particle. There was not information available that measured the ratios within the aerosol, so two different compositions were considered. The first composition is that the aerosol is entirely organic which will provide a conservatively low κ value. The second composition is a mixture of salts and organics that match the ratios in the SML samples. This will provide a conservatively high κ value. It is expected that our κ values calculated for the ambient CCN aerosol would fall between these different composition scenarios. The critical diameter will again come from the CCN measurements (to match the critical diameters used in determining κ values from CCN measurements) but the critical supersaturation will be calculated using chemical composition data from the two different scenarios being considered.

3.1. Calculating κ Values from CCN Measurements

To measure κ from the CCN measurements the critical diameter and the critical supersaturation are needed. The ratio of the concentration of particles which activate at a given supersaturation

as CCN to the total concentration of particles counted is the activated fraction. Plotting the activated fraction against the dry diameter and determining the diameter at which 50% of the particles are able to activate provides the critical diameter.

$$\text{Activated fraction} = \frac{\text{concentration of particles which activate as CCN}}{\text{total concentration of aerosols}} \quad (1)$$

The critical supersaturation is the supersaturation being measured by the CCN instrument at the time the critical diameter is being measured. Due to instrument inaccuracies the supersaturation set on the CCN instrument may not be the exact supersaturation being measured within the CCN instrument. Using calibration data the supersaturation set in the CCN instrument can be adjusted to match the supersaturation being measured within the CCN instrument. Using data from an ammonium sulfate calibration, the critical supersaturation determined using Köhler Theory can be plotted against the delta temperature measured within the CCN instrument. Then finding the equation of the line, the delta temperature from the CCN instrument can be used to calculate an adjusted supersaturation. This adjusted supersaturation measured within the CCN instrument is the critical supersaturation. Once the critical diameter (D) and critical supersaturation (S_c) are known the κ value can be determined for the CCN measurements using Equations 2 and 3 (Petters & Kreidenweis, 2007). In these equations σ_{water} is the surface tension of the water, MW_{water} is the molecular weight of water, ρ_{water} is the density of water, R is the ideal gas constant, T is the temperature in Kelvin, D is the dry diameter of the particle, and S_c is the critical saturation ratio. The terms within the variable A are based on pure water. This includes the assumption that the surface tension of the droplet is equal to the surface tension of pure water.

$$A = \frac{4\sigma_{water}MW_{water}}{\rho_{water}RT} \quad (2)$$

$$\kappa = \frac{4A^3}{27D^3\ln(S_c)^2} \quad (3)$$

3.2. κ Calculations Including Chemical Composition Data

3.2.1. Organics Selected for Calculations

To provide further insight on specific organic groups present in the samples, the κ values were predicted based on the size and chemical composition of the aerosols. Several of the parameters needed for calculating κ are influenced by composition changes within the water affected by the measured concentrations of salts and total organic carbon. In order to predict a κ value using composition data, assumptions must be made about the organics present in the SML samples. Seven different organic compositions of humic acid, fulvic acid, glucose, 6-glucose, RuBisCO, chlorophyll *a*, and triolein, were chosen to calculate the predicted κ values of the samples. κ values were determined for each organic individually (DSML samples) and for mixtures of the organic and salts (assuming artificial seawater salts in SML samples). To determine the ratio of organics to inorganics the TOC concentrations and salinity are used. These κ values were compared to the κ values from the CCN measurements.

The organics selected for the analysis cover various organics common in aerosols and ocean waters. Humic acid and fulvic acid are considered representative organic compounds in aerosol samples. Humic acid and fulvic acid are known to contribute significantly to dissolved organic matter (DOM) and to surfactant concentration, both of which can become enriched in the SML

(Drozdowska et al., 2017). In the desalinated sea surface microlayer samples, the presence of free glucose was unlikely to be significant. The molecular weight cutoff (MWCO) of the dialysis tubing was 1,000 Daltons and the molecular weight of glucose is 180 Daltons. Glucose would have been able to escape the dialysis tubing with the salts during the desalination process. However, glucose was selected since it is a major component of DOM and a main building block of polysaccharides. Since the presence of free glucose in the desalinated samples was unlikely, a 6-glucose organic compound was also considered for the organic composition. This compound is large enough to remain within the dialysis tubing during the desalination process but is composed of glucose molecules which are known to be commonly found in DOM. Ribulose-1,5-bisphosphate carboxylase/oxygenase (RuBisCO) was also selected to represent the organic composition when predicting κ values. RuBisCO is the most abundant protein on Earth (Ellis, 1979). RuBisCO is a key enzyme in carbon fixation in aquatic plants, algae, cyanobacteria, and phototropic and chemoautotrophic bacteria, and is responsible for 95% of marine photosynthesis (Orellana & Hansell, 2012). Photosynthesis will occur throughout the euphotic zone and some of the hydrophobic or surface-active compounds could partition to the SML. This could lead to an increase in the amount of RubisCO present in the SML. In the uppermost surface waters (including the SML) the rate of photosynthesis could be lower because there is too much light and the UV light is destructive but overall the rate of photosynthesis is higher in the upper layers of the ocean than the subsurface waters. For marine SML samples another choice for the organics present was chlorophyll *a*. During the NAAMES campaigns measurements of the chlorophyll *a* concentrations were made. In some cases, the intensity of microbe-derived organics was positively correlated with an air mass that had been exposed to phytoplankton biomass as proxied by chlorophyll (Choi et al.). Lastly, triolein was chosen to represent the

organics present in the SML. In unpolluted surface microlayers 40-65% of the lipids are fatty acids and triacylglycerols (Arts, 1999). Triolein is a triglyceride that is formed from oleic acid. Oleic acid has been measured in the North Atlantic Ocean waters and also from aerosol measurements sampled over the North Atlantic Ocean (Duce et al., 1983). Properties for each of the organic compounds assumed to determine a κ value are shown in Table 2.

Table 2. Properties of organic compounds

Organic Compound	Molecular Weight (g/mol)	Density (g/cm ³)	Number of Carbons	κ
Humic Acid	2,000.0	1.57	84	0.014
Fulvic Acid	500.0	1.47	14	0.053
Glucose	180.2	1.53	6	0.15
6-Glucose	1,080.9	1.5	36	0.025
RuBisCO	560,000.0	1.6	3,025	5.16E-05
Chlorophyll <i>a</i>	893.5	1.079	55	0.022
Triolein	885.4	0.915	57	0.019

3.2.2. Calculating κ Based on Chemical Composition Data

To calculate a κ value for the compositions discussed above several steps are needed. The first step in calculating a κ value is determining the concentration of salts from the salinity. The salinity was measured prior to the desalination process using a portable refractometer. In order to calculate the concentration of salts, the molecular weight of the solution (artificial seawater salts and water) and the density of the solution must be determined following the method described in Equations 4-6. In these equations $MW_{solution}$ is the molecular weight of the solution, n_{salts} is the number of moles of salts in artificial seawater, n_{total} is the total number of moles in the solution, MW_{salts} is the weighted molecular weight of salts in artificial seawater, MW_{water} is the

molecular weight of water, $\rho_{solution}$ is the density of the solution, ρ_{salts} is the weighted density of salts in artificial seawater, and ρ_{water} is the density of water.

$$MW_{solution} = \left(\frac{n_{salts}}{n_{total}}\right) MW_{salts} + \left(1 - \left(\frac{n_{salts}}{n_{total}}\right)\right) MW_{water} \quad (4)$$

$$\rho_{solution} = \left(\frac{n_{salts}}{n_{total}}\right) \rho_{salts} + \left(1 - \left(\frac{n_{salts}}{n_{total}}\right)\right) \rho_{water} \quad (5)$$

$$salt\ concentration\ \left(\frac{g}{L}\right) = salinity(parts\ per\ thousand) \quad (6)$$

Once the concentration of salts is known the next step is determining the concentration of total organic carbon. The concentration of TOC is based on the number of carbons located within the organic compound. Each organic compound was treated individually in a separate calculation to determine the organic concentration for that single compound. Equation 7 shows how to calculate the organic concentration. This equation assumes that the ratio of organic carbon to organic matter is 1:1. In this equation the TOC concentration was provided in $\left(\frac{\mu mol\ C}{L}\right)$, which is the number of μ moles of carbon per liter, N is the number of carbon atoms in the chosen organic compound, and MW_{org} is the molecular weight of the chosen organic compound.

$$organic\ concentration\ \left(\frac{g}{L}\right) = (TOC\ concentration) \left(\frac{1}{10^6}\right) \left(\frac{1}{N}\right) (MW_{org}) \quad (7)$$

Since the SML samples contain both salts and organics, the next step is to determine the volume weighting factors for the SML aerosols. These volume weighting factors were determined following the work by Petters et al. (Petters & Kreidenweis, 2013). In calculating the volume

weighting factors it was assumed that the volume of the solute plus the volume of water equals the total volume (volume additivity assumption) which allows using the pure water density to determine the partial molar volume of water. One weighting factor will be used to determine the amount of salts present in the aerosol and the other weighting factor will be used to determine the amount of organics present in the aerosol. In these equations W_i is the volume weighting factor for the inorganics, W_o is the volume weighting factor for the chosen organic compound, *salt concentration* is the amount of salts in the sample determined using Equation 6, ρ_{salts} is the weighted density of salts in artificial seawater, *organic concentration* is the amount of organic in the sample determined using Equation 7, and ρ_{org} is the density of the chosen organic compound.

Volume weighting factors

$$W_i = \frac{\frac{\textit{salt concentration}}{\rho_{salts}}}{\frac{\textit{salt concentration}}{\rho_{salts}} + \frac{\textit{organic concentration}}{\rho_{org}}} \quad (8)$$

$$W_o = \frac{\frac{\textit{organic concentration}}{\rho_{org}}}{\frac{\textit{salt concentration}}{\rho_{salts}} + \frac{\textit{organic concentration}}{\rho_{org}}} \quad (9)$$

In addition to calculating the volume weighting factors the molar weighting factors are also calculated for both the inorganics and the organics present in the SML aerosols. In these equations $W_i\textit{mole}$ is the molar weighting factor for the inorganics, $W_o\textit{mole}$ is the molar weighting factor for the chosen organic compound, *salt concentration* is the amount of salts in the sample determined using Equation 6, MW_{salts} is the weighted molecular weight of salts in

artificial seawater, *organic concentration* is the amount of organic in the sample determined using Equation 7, and MW_{org} is the molecular weight of the chosen organic compound.

Molar weighting factors

$$W_i mole = \frac{\frac{\textit{salt concentration}}{MW_{salts}}}{\frac{\textit{salt concentration}}{MW_{salts}} + \frac{\textit{organic concentration}}{MW_{org}}} \quad (10)$$

$$W_o mole = 1 - W_i mole \quad (11)$$

The density of the particle is determined using the volume weighting factors. In this equation $\rho_{particle}$ is the density of the particle, W_i is the volume weighting factor for inorganics, ρ_{salts} is the weighted density of salts in artificial seawater, W_o is the volume weighting factor for organics, and ρ_{org} is the density of the chosen organic compound.

$$\rho_{particle} = W_i \rho_{salts} + W_o \rho_{org} \quad (12)$$

Similarly, the mass of the organic in the SML aerosol is determined using the density of the organic and the volume of the particle. In this equation $mass_{organic}$ is the mass of the organic, ρ_{org} is the density of the organic, and V is the volume of the particle.

$$mass_{organic} = \rho_{org} V \quad (13)$$

Once the density of the particle is known, the mass of the mixture within the SML particle can be calculated. In this equation $mass_{mixture}$ is the mass of the mixture, $\rho_{particle}$ is the density of the particle determined using Equation 12, and V is the volume of the particle.

$$mass_{mixture} = \rho_{particle}V \quad (14)$$

Since the SML aerosol is a mixture of inorganics and organics the factors to calculate a κ for the aerosol must be weighted based on the amount of inorganics and organics present in the aerosol. These variables include a weighted van't Hoff factor and a weighted molecular weight. In these equations $i_{weighted}$ is the weighted van't Hoff factor for the mixture, W_{imole} is the molar weighting factor for the inorganics, i_{salts} is the weighted van't Hoff factor for salts in artificial seawater, W_{omole} is the molar weighting factor for the organics, i_{org} is the van't Hoff factor for the organic, $MW_{weighted}$ is the weighted molecular weight for the mixture, MW_{salts} is the weighted molecular weight of salts in artificial seawater, and MW_{org} is the molecular weight of the chosen organic compound.

Weighted van't Hoff factor

$$i_{weighted} = W_{imole}(i_{salts}) + W_{omole}(i_{org}) \quad (15)$$

Weighted molecular weight

$$MW_{weighted} = W_{imole}(MW_{salts}) + W_{omole}(MW_{org}) \quad (16)$$

In order to calculate κ two additional variables must be calculated, b and c (North & Erukhimova, 2009). The equations for determining parameters b and c are shown in Equations 17-18. Equation 17 does not include chemical composition data. In this equation $\sigma_{measured}$ is the measured surface tension of the sample, ρ_{water} is the density of water, R is the ideal gas constant, and T is the temperature in Kelvin.

$$b = \frac{2\sigma_{measured}}{\rho_{water}RT} \quad (17)$$

In calculating the parameter c , the weighted factors calculated above are needed. For the SML aerosols containing both inorganics and organics the weighted factors adjust the calculations to reflect the amounts of inorganics and organics present in the mixed aerosol. When determining κ for the aerosols generated by the desalinated SML samples, the weighted factors are also needed, even though the desalination process was effective salts remained. Therefore, the aerosols generated by the DSML samples must also be treated as a mixture of salts and organics but the amount of salts has been greatly reduced. When the aerosol was treated as organic only, the κ values predicted were too low and did not match the κ values calculated using the CCN measurements. Equation 18 includes chemical composition data that is needed to calculate a κ value for the aerosols generated by the SML and DSML samples. Equation 18a and 18b show how the equation is modified depending on if the aerosol is mixed (inorganics and organics) or considered pure organic. In these equations c is a parameter, i is the van't Hoff factor, $mass_s$ is the mass of the solute, MW_{water} is the molecular weight of water, ρ_{water} is the density of water, MW_s is the molecular weight of the solute, c_o is a parameter for organic composition only, i_{org} is the van't Hoff factor for the organic, $mass_{organic}$ is the mass of the organic, MW_{org} is the molecular weight of the chosen organic compound, c_m is a parameter for a mixture of organics and inorganics, $i_{weighted}$ is the weighted van't Hoff factor, $mass_{mixture}$ is the mass of the mixture, and $MW_{weighted}$ is the weighted molecular weight. The mixture mass will either be the organics plus the salts measured before desalination (salinity measurements) or the mixture mass

will be the organics plus the salts measured after desalination (ion chromatography measurements).

$$c = \frac{3i(mass_s)(MW_{water})}{4\pi\rho_{water}MW_s} \quad (18)$$

$$c_o = \frac{3(i_{org})(mass_{organic})(MW_{water})}{4\pi\rho_{water}MW_{org}} \quad (18a)$$

$$c_m = \frac{3(i_{weighted})(mass_{mixture})(MW_{water})}{4\pi\rho_{water}MW_{weighted}} \quad (18b)$$

In Equation 19 b and c are the parameters calculated in Equations 17 and 18, SR is the critical saturation ratio, and S_c is the critical supersaturation.

Critical saturation ratio is defined as:

$$SR = 1 + \sqrt{\frac{4b^3}{27c}} \quad (19)$$

Critical supersaturation is defined as:

$$S_c = (SR - 1)100 \quad (20)$$

After the critical saturation ratio has been calculated, it is used in variations of Equations 2 and 3 to determine the κ values. In Equations 2b and 3b, the surface tension was measured from the samples and was not the surface tension of pure water. These κ values reflect the chemical composition data used based on which organic is assumed to be in the SML sample. Each

organic was treated as an independent case and the entire organic composition was assumed to be of a single compound. The salts used in the calculations were assumed to be the salts in artificial seawater.

$$A = \frac{4\sigma_{measured}MW_{water}}{\rho_{water}RT} \quad (2b)$$

$$\kappa = \frac{4A^3}{27D^3\ln(S_c)^2} \quad (3b)$$

3.2.3. Calculating κ for Ambient Aerosol Data

The next step in the analysis was to calculate κ values from the ambient CCN aerosol measurements. During the NAAMES campaigns a condensation particle counter (CPC) measured the total concentration of particles and a CCN counter measured the concentration of particles which activated at a specific supersaturation. The supersaturations measured were 1.50%, 1.20%, 0.90%, 0.70%, 0.50%, 0.35%, 0.25%, 0.15%, and 0.05%. By comparing κ values from the ambient CCN aerosol data to the κ values from the SML samples, a connection could be made proving that the aerosols created from the SML were lofted into the air and measured as ambient CCN aerosols. If the κ values are similar between the SML samples and the ambient aerosols then the argument could be made that due to windy conditions and wave breaking, the SML aerosols were being lofted into the atmosphere and being measured as the ambient aerosols. It is important to note that during the NAAMES 3 field campaign the CCN instrument located on the ship experienced issues and was unable to collect data during the final days at station 6. Since one of the SML samples being analyzed was collected during this time, the last available CCN data collected on station 6 was used for this analysis. While the aerosols

measured during this time would not have been identical to aerosols present during the SML collection, it is the closest CCN data available. It was important to perform this analysis with another sample from the NAAMES 3 campaign to compare to the two samples from the NAAMES 4 campaign.

In order to calculate κ values from the ambient aerosol data the size of the aerosols must be determined. The data from the CCN during the times of SML sampling was unsized. By using the scanning electrical mobility sizer (SEMS) data it is possible to determine what the critical diameter of the aerosol would have been at each supersaturation during SML sampling. These calculations are outlined below based on the previous work of Moore et. al (R. H. Moore et al., 2011; Moore et al., 2012). First the SEMS data had to be converted to concentration in number per cubic centimeter from normalized concentration. In this equation $D_{p(i+1)}$ is the diameter of the next largest size bin, $D_{p(i)}$ is the diameter of the size bin that will be unnormalized, and N_i is the normalized SEMS concentration.

$$SEMS \text{ concentration } \left(\frac{\#}{cm^3} \right) = \left(\frac{1}{D_{p(i+1)} - D_{p(i)}} \right) (N_i) \log_{10} \left(\frac{D_{p(i+1)}}{D_{p(i)}} \right) \quad (21)$$

To determine the CCN concentrations needed for calculating the κ values for the ambient aerosol, the times that the microlayer was being sampled were matched to CCN concentrations. The microlayer sampling occurred over an hour-long period where the CCN concentrations were measured at each supersaturation once. The CCN concentration used for the analysis was averaged over the last minute of collection at each supersaturation to ensure that the CCN was reliably measuring that supersaturation. Since the ambient CCN aerosol data measured on the

ship did not have an associated size, the SEMS data was used to calculate the aerosol size. With the concentration of particles able to activate as CCN at a specific time and supersaturation, the same time was identified in the SEMS data. By integrating under the SEMS data beginning from the largest size bin and integrating toward smaller size bins, the total concentration of particles in a size range was calculated. Making the assumption that all particles larger than the critical diameter will activate as CCN, then the critical diameter of the aerosol population is the lower bound of integration where the number of particles measured by the SEMS is equal to the concentration of particles able to activate as CCN. To determine the area under the SEMS size distribution, the trapezoid method was utilized. In this equation $A_{trapezoid}$ is the area of a trapezoid, $base_1$ is the concentration at the upper size bin, $base_2$ is the concentration at the lower size bin, and h is the difference between the upper size bin and the lower size bin.

$$A_{trapezoid} = \left(\frac{base_1 + base_2}{2} \right) h \quad (22)$$

This methodology does include the assumption that once that critical diameter is reached all of the particles larger than this size will activate as CCN. Once this critical diameter is known Equations 2 and 3 can be used to find the κ values for the ambient aerosols. In these calculations the supersaturation is the supersaturation being measured by the CCN instrument during the measurements.

3.2.4. Calculating κ for Ambient CCN Aerosol Including Composition Data

Once the most representative organic composition was determined from the predicted κ values from the SML and DSML samples, this composition can be included in predicting a κ value for

the ambient CCN aerosols. The exact ratio of organics to salts is unknown in the aerosol but using the organic composition of RuBisCO the upper and lower limits for κ can be determined assuming two different compositions, an organic only (lower κ bound) composition and a RuBisCO and salt mixture (upper κ bound). The lower bound for the ambient CCN aerosol κ value would be to assume the entire aerosol was composed of only RuBisCO. The upper bound for the aerosol κ value of the aerosol would be to assume the composition is identical to the ratio of salts to inorganics in the SML samples. Realistically, the composition in the ambient CCN aerosols would fall somewhere between these two limits.

In Equation 24 the weighted van't Hoff factor, density, and molecular weight were calculated using the same equations listed above. In these equations κ is the hygroscopicity parameter, i_{org} is the van't Hoff factor for the organic, ρ_{org} is the density of the organic, MW_{water} is the molecular weight of water, ρ_{water} is the density of water, MW_{org} is the molecular weight of the organic, $i_{weighted}$ is the weighted van't Hoff factor for the mixture, $\rho_{weighted}$ is the weighted density of the mixture, and $MW_{weighted}$ is the weighted molecular weight of the mixture.

Lower limit κ for ambient aerosol

$$\kappa = \frac{i_{org}\rho_{org}MW_{water}}{\rho_{water}MW_{org}} \quad (23)$$

Upper limit κ for ambient aerosol

$$\kappa = \frac{i_{weighted}\rho_{weighted}MW_{water}}{\rho_{water}MW_{weighted}} \quad (24)$$

4. RESULTS

4.1. TOC

The station averaged TOC concentrations in the SML samples are shown in Figure 9. These concentrations were used to calculate the amount of organics present in the aerosols generated by the SML and DSML samples. The chlorophyll *a* concentrations at these stations is also shown. The highest and lowest chlorophyll *a* stations for each cruise were selected for the desalination process.

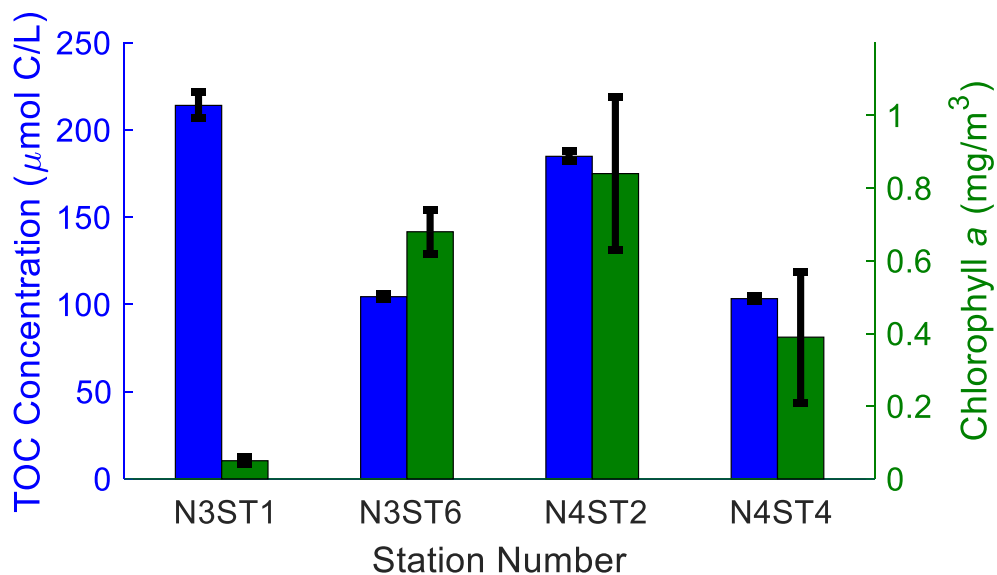


Figure 9. Station averaged TOC concentration in SML samples

4.1.1. Amino Acid Analysis

From the amino acid analysis, additional information on the organics was determined. In Figure 10 the amounts of total dissolved amino acids (TDAA) in the SML samples are compared to the

TDAA in the subsurface waters, it is evident that there were higher yields in the SML samples. Since TDAA comprises a large portion of freshly produced DOM that can be readily utilized by microbes, these higher yields suggest that the DOM in the SML samples was more recently produced than the DOM in the subsurface waters. Figure 11 shows the mole percentage of beta-alanine and gamma-aminobutyric acid (GABA) present in the SML samples and the subsurface water. In this data the concentrations are lower in the SML samples which suggests that the DOM in the SML samples was less diagenetically altered. This reinforces the results presented in Figure 10 showing that the DOM present in the SML is fresher than the DOM in the subsurface waters. TDAA yields are considered the most effective indicators for early diagenesis and GABA is considered the most effective indicator of advanced DOM diagenesis (Davis, Kaiser, & Benner, 2009).

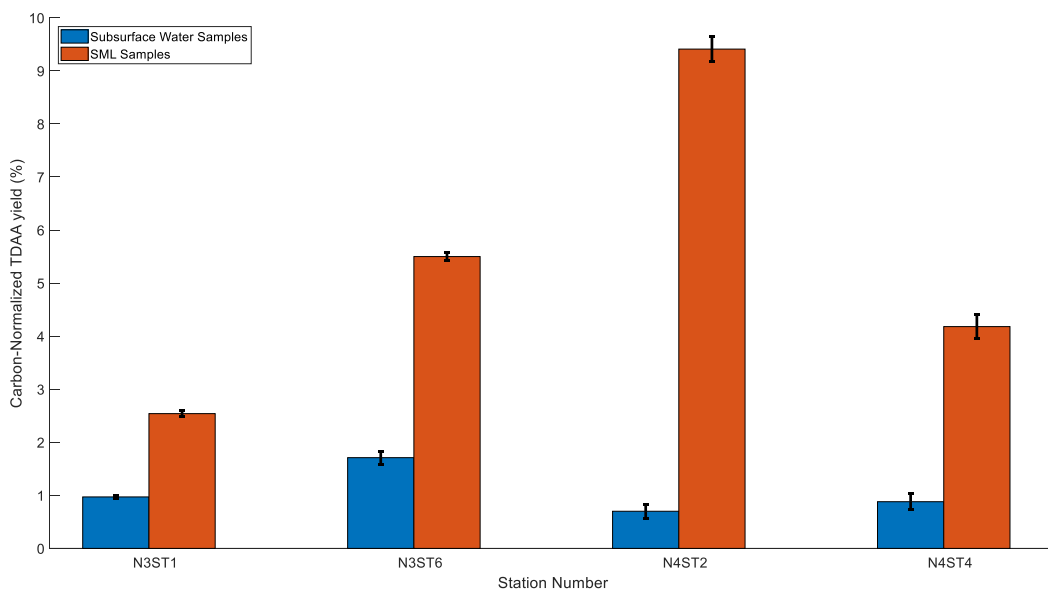


Figure 10. Total dissolved amino acids (TDAA) in SML samples and subsurface water samples

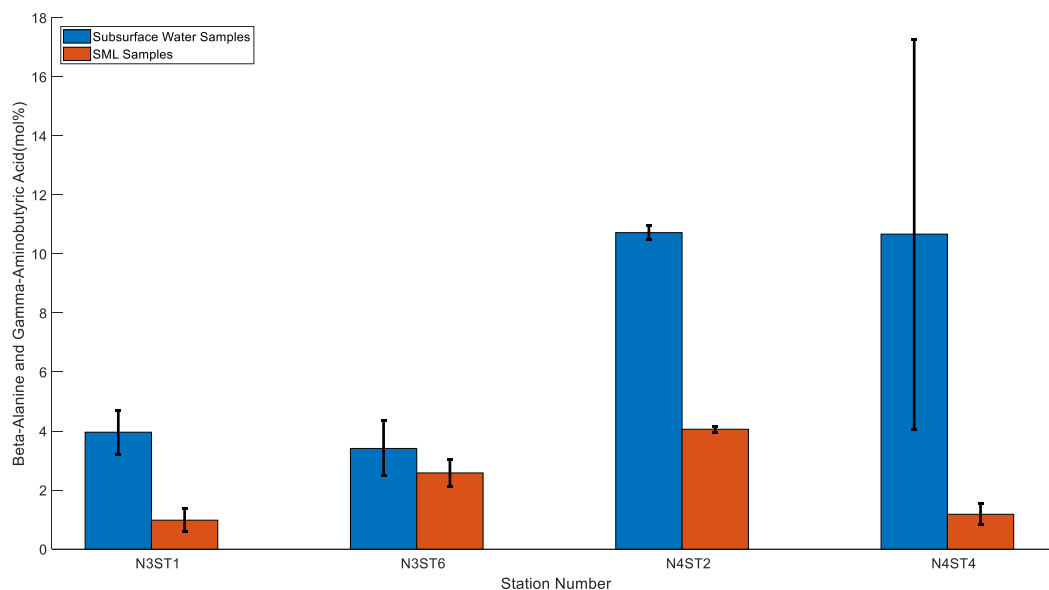


Figure 11. Beta-alanine and gamma-aminobutyric acid (GABA) in SML samples and subsurface water samples

The values shown are the combined mol % of beta-alanine and gamma-aminobutyric acid.

The labile DOM in the SML could be produced by the phytoplankton population. The size of organic matter can be related to its diagenetic state. A decrease in the size of DOM suggests increasing diagenesis and chemical alteration (Amon & Benner, 1996; Amon, Fitznar, & Benner, 2001). Cowie and Hedges (1994) found that carbon-normalized amino acid yields were the most effective during the early stages of degradation while significant increases in the mol% of beta-alanine and gamma aminobutyric acid (GABA) only occurred in higher altered, older samples (Cowie & Hedges, 1994). Freshly produced DOM with elevated concentrations of carbon-normalized amino acid yields are indicative of labile material (Davis & Benner, 2007). This information was considered when choosing difference organic compositions to use when predicting a κ value. The choices for larger organic material can be justified by the fact that the DOM in the SML was more labile and should contain larger material. This also suggests that the

desalination process was likely not removing the bulk of the DOM. While the dialysis tubing allowed the majority of the salt to leave the samples, due to the pore size of the tubing the smaller organics could also be removed. These results provide information to suggest that the organics remaining in the SML samples after desalination were representative of the organics present in the original SML samples.

4.2. Results from Measurements Made at NASA Langley Research Center

4.2.1. WIBS

The WIBS provided evidence of biological material present in the aerosolized SML and DSML samples. Figure 12 shows the results from analyzing the aerosols generated by the SML and DSML samples using the WIBS.

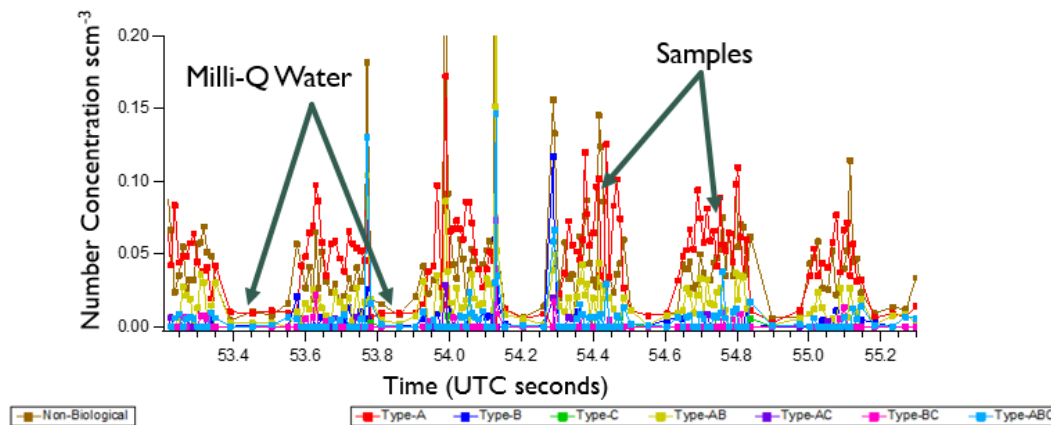


Figure 12. Analysis of the aerosols generated by SML and DSML samples using the WIBS

When analyzing the SML and DSML samples using the WIBS, Milli-Q water was used as a blank between samples. It is known that the Milli-Q water should not contain any material that would fluoresce with the WIBS, therefore the number of fluorescing particles should drop to

zero when the Milli-Q water was running through the system. This was shown in the data indicating that the system was able to recognize the change in composition between the SML and DSML samples to the Milli-Q water. In each of the SML and DSML samples the particles were able to fluoresce (majority type A). Type A particles are excited at a wavelength of 280 nm. The 280 nm band was used to excite the specific target biological molecule tryptophan that may be present within the particle. Both SML and DSML fluorescing particles were categorized as type A, this shows that the desalination process did not cause a shift in the type of particle fluorescence. Since the WIBS was able to measure a signal of fluorescence from all SML and DSML samples, this showed the presence of targeted bioaerosol markers. This indicated the influence of biology through organic aerosols in all samples.

4.2.2. Ion Chromatography

By comparing the concentrations of inorganics measured before and after the desalination process, it was clear that the desalination method used on the SML samples was effective. The amount of NaCl removed in the SML samples from the desalination process was a minimum of 99.95% reduction. Figure 13 shows a comparison between the salt concentrations measured using the portable refractometer and the ion chromatography data.

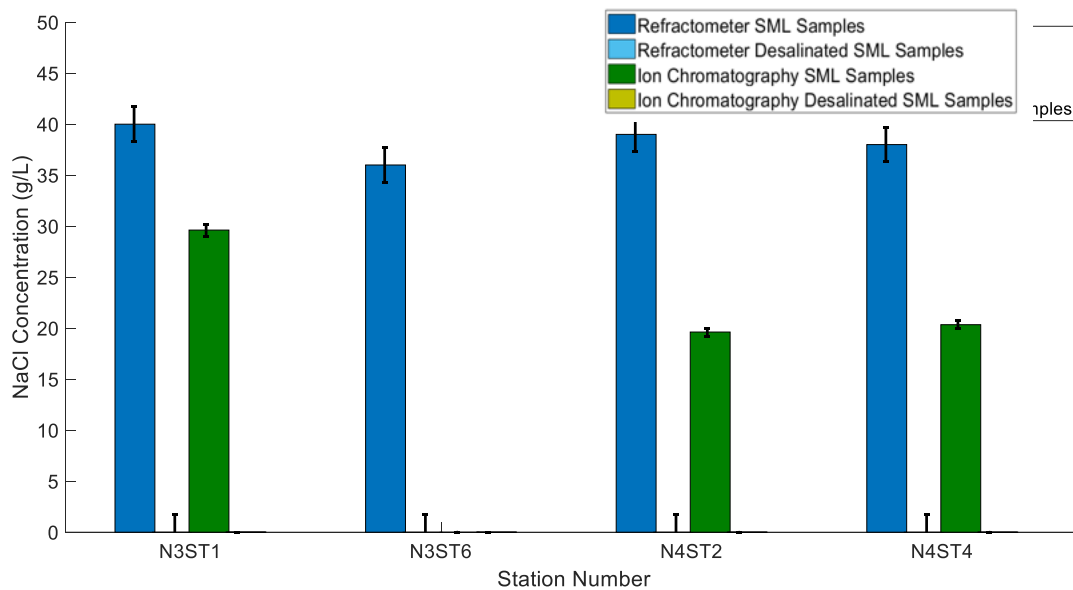


Figure 13. Reduction in NaCl concentration in SML samples from portable refractometer and ion chromatography data

4.2.3. Surface Tension

Measuring the surface tension of the SML and DSML samples did show variation from the surface tension of pure water (72.8 mN/m). In order to have an effect on the ability to predict CCN, the depression in the surface tension of the samples would have had to be much larger than what was measured. For accuracy in the calculations the surface tension measured from the samples was used in the calculations for κ . The measured surface tension values were utilized in Equations 2b, 3b, 17, and 19 to determine the critical saturation ratio which is used when predicting κ values for the aerosols generated by the SML and DSML samples. Figure 14 shows the surface tension measurements used in the predicted κ calculations.

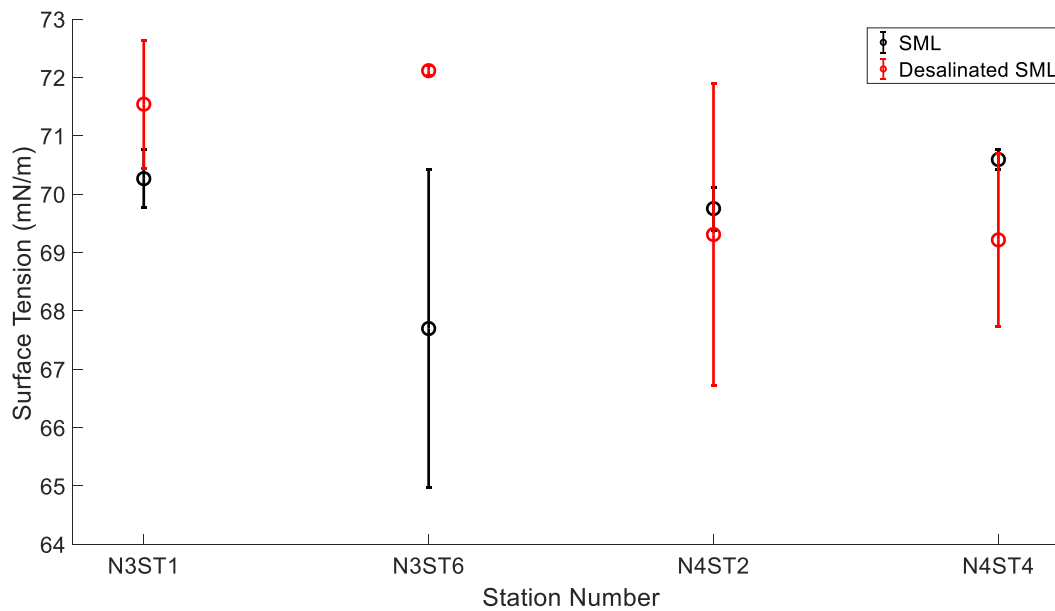


Figure 14. Surface tension measurements of SML and DSML samples

Additionally, the surface tension measurements were analyzed using SigmaPlot software to determine if the surface tension measurements were significantly different than the surface tension of pure water. The SigmaPlot report results are included in Appendix B. The analysis used was a one way analysis of variance. Since the measurements did not have a normal distribution, the Shapiro-Wilk Normality Test failed. The analysis was then changed to a Kruskal-Wallis one way analysis of variance on ranks. This method compares the median of three different groups where the groups can be of unequal size and the distributions are assumed to be of the same shape. The three groups used in the comparison are the measurements of pure water, SML samples, and DSML samples. From the Kruskal-Wallis method the difference in the three median values among the sample types was greater than would be expected by chance. Meaning there is a statistically significant difference between the medians of the three sample types. To compare between the three different sample groups Dunn's Method was used. Dunn's

Method is a non-parametric pairwise multiple comparisons procedure based on rank sums. It is commonly used after the rejection of a Kruskal-Wallis test. It allows for multiple pairwise t-tests following the rejection of a one way analysis of variance null hypothesis. From Dunn's method it was determined that there was a significant difference between the surface tension of pure water and the surface tension of the SML samples. There was not a significant difference between the surface tension of pure water and the surface tension of the DSML samples. There was a significant difference between the surface tension of the SML samples and the surface tension of the DSML samples. From these data it would appear that the large amount of salt present in the SML samples caused a difference in surface tension compared to pure water. Since the DSML samples were not significantly different, this would indicate that the reduction of salts, and other small compounds lost during desalination, in these samples was unable to affect the surface tension. It is unclear from these results how the organics were contributing to the difference in surface tension between sample types. Since the SML samples had surface tension that was significantly different than pure water, including the actual surface tension measurements in the calculations was more representative than assuming the surface tension of pure water.

4.2.4. CCN

Analyzing the aerosols generated from the SML and DSML samples showed that the samples containing a higher concentration of salts were more hygroscopic than the samples that had undergone the desalination process. The samples that had undergone desalination had a lower κ value which confirmed that decreasing the amount of salts while largely maintaining the organics present in the samples decreased the κ value of aerosols generated by the samples. The aerosols generated by the SML samples had κ values of 0.96 ± 0.12 and the aerosols generated by the

DSML samples had κ values of 0.36 ± 0.05 . This indicated that the κ values for the SML samples are driven largely by the presence of salts. Figure 15 shows how the aerosols generated by the SML and DSML samples varied by station. From this figure it was apparent that there is a shift in the critical diameter size from the SML samples to the DSML samples. The larger critical diameters from the DSML samples could be justified by the fact that smaller compounds (molecules less than 1000 Daltons) were lost during the desalination process and this could lead to having larger compounds remaining in the samples.

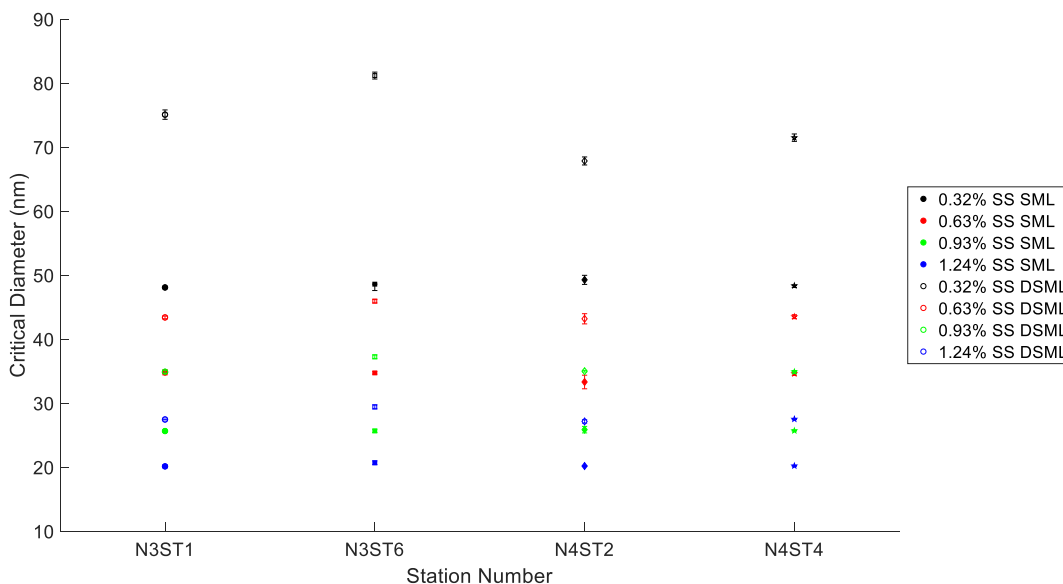


Figure 15. Critical diameter by station for aerosols generated by SML and DSML samples
Each color represents measurements taken at a different supersaturation.

Figure 16 shows the κ values for the SML and DSML samples by station. Due to the larger concentration of salt present in the SML samples, the κ values of the SML samples would be expected to be larger than the κ values for the DSML samples. Reducing the salt concentration in the DSML samples significantly lowers the κ values for the samples.

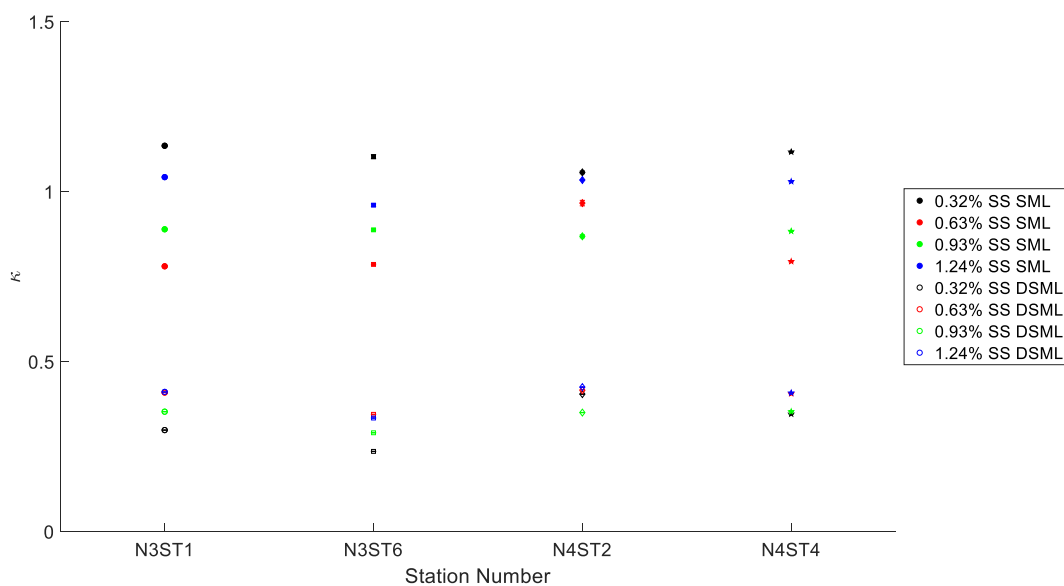


Figure 16. κ by station for aerosols generated by SML and DSML samples
 Each color represents measurements taken at a different supersaturation.

Figure 17 shows κ values derived from the CCN measurements of the aerosols generated by the SML and DSML samples. These κ values indicate that the SML samples containing the larger concentration of salts have a higher κ value than the DSML samples which contain a reduced concentration of salts. Since salts are known to produce effective κ values, these results confirm the κ values are driven by the salt concentration in the samples.

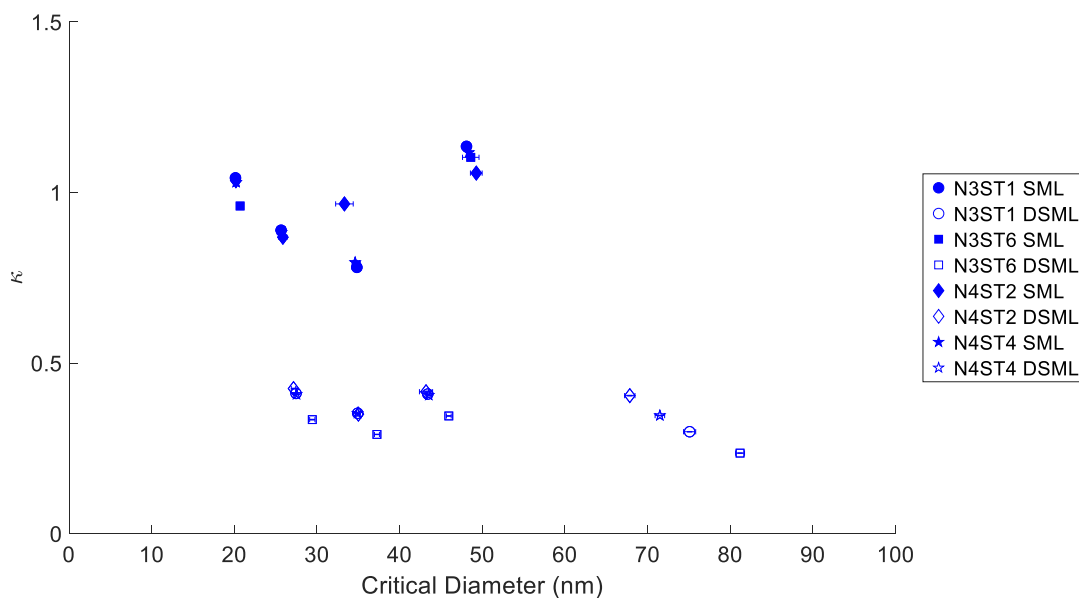


Figure 17. κ calculated from CCN measurements

The filled in shapes correlate to sea surface microlayer samples and the empty shapes correlate to the desalinated sea surface microlayer samples. The different shapes represent the different stations where the samples were collected.

When discussing aerosols generated in a marine environment, the κ values for the aerosol are often compared to the κ values of artificial seawater and sodium chloride. The κ value for sodium chloride, 1.28, was determined assuming that the composition was pure and not composed of a mixture; while the κ value for artificial seawater, 1.1, was determined using lab experiments (Zieger et al., 2017). Figure 18 shows these reference κ values for salts with the κ values calculated from the CCN measurements. When comparing these κ values, the κ values from the SML samples fall below sodium chloride and only slightly below the artificial seawater κ values. This implies that the aerosols generated by the SML would be considered effective cloud formers with κ values 0.96 ± 0.12 . In contrast, the aerosols generated by the DSML samples would be considered less effective at forming clouds with κ values of 0.36 ± 0.05 . For comparison, another field campaign calculated marine κ values of 0.65 (Atwood et al., 2017). In

a study comparing field and laboratory measurements Collins et al. determined a marine κ value of 0.95 ± 0.15 (Collins et al., 2016). The κ values calculated based on the CCN measurements are also in agreement with the global marine κ value stated by Pringle et al. of 0.72 ± 0.24 (Pringle et al., 2010). In both Figure 17 and Figure 18 the κ values vary across the SML samples and across the DSML samples. This implies that there is a composition change between the samples at each station. If the composition was uniform in each sample then the κ value being calculated would also be uniform for each sample.

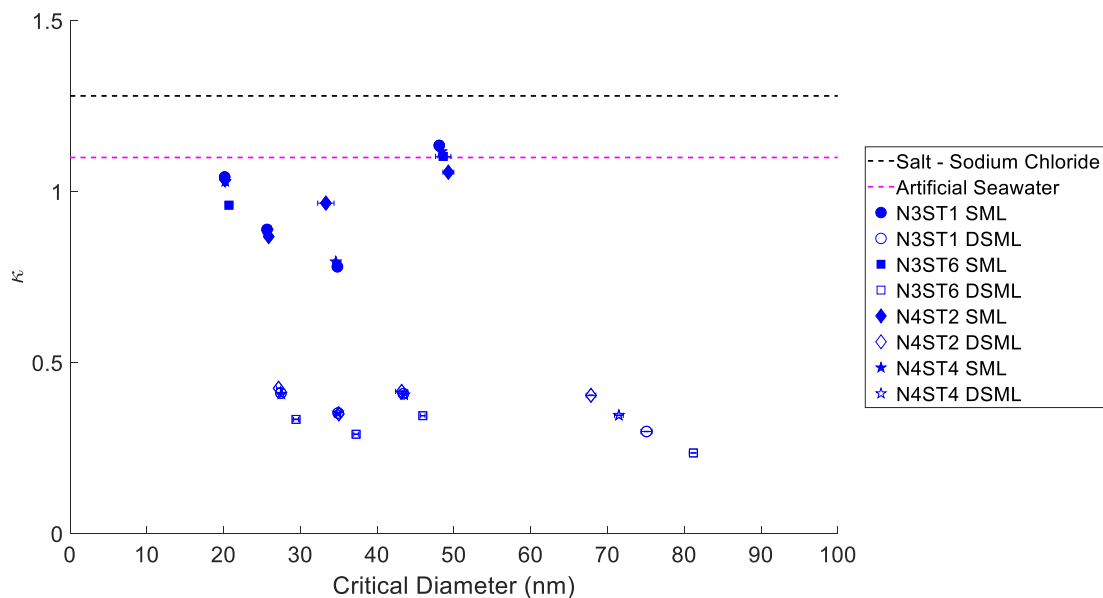


Figure 18. κ calculated from CCN measurements and κ for reference salts

The filled in shapes correlate to sea surface microlayer samples and the empty shapes correlate to the desalinated sea surface microlayer samples. The different shapes represent the different stations where the samples were collected. The black dashed reference line indicates the κ value for pure sodium chloride. The magenta dashed reference line indicates the κ value for artificial seawater.

4.2.5. Varying Organic Type in κ Calculation

Figure 20 shows the κ values from the CCN measurements compared to the κ values from predictions including chemical composition data for the SML samples. When using the sizes

measured from the aerosols generated by the SML samples and adjusting the organic composition, there is no noticeable difference between organic type used. All of the predicted κ values appear to have almost an identical κ value. Taking the standard deviation of the κ values predicted for the SML samples across all of the different organic composition scenarios provides at most 0.004 variation in κ . This small variation across different organic compositions used was due to large amounts of salt present in the SML samples. The small amount of organic in these samples cannot make a significant contribution due to the amount of salt. All of these κ values predicted for the SML samples are similar to the κ value for pure sodium chloride, 1.28. This demonstrated how much the salt was driving the κ value versus the contribution from the organics. Figure 20 shows the κ values from the CCN measurements and the predicted κ values for the DSML samples. With the κ values predicted for the DSML samples it was clear that there was a difference between the different organic compositions used. In this first set of predictions the DSML composition was assumed to be entirely organic due to the efficiency of the desalination process. With these κ predictions it was apparent that the organic composition influenced the κ value for the aerosol. Taking the standard deviation of the κ values predicted for the DSML samples across all of the different organic composition scenarios provides at most 0.05 variation in κ . This variation is ten times higher than the variation seen in the SML samples across different organic composition scenarios. In these samples the salt reduction allowed the contribution from the organics to be better quantified.

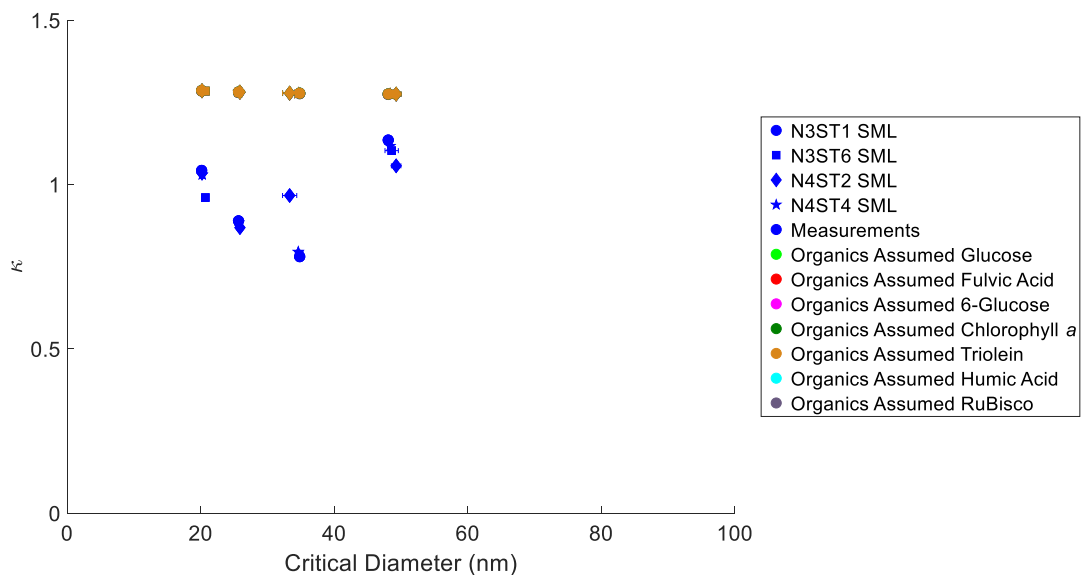


Figure 19. Measured and predicted κ values for SML samples

The filled in shapes correlate to sea surface microlayer samples and the different shapes represent the different stations where the samples were collected. The dark blue markers indicate the κ values calculated from direct CCN measurements. The other colored markers are for a predicted κ value assuming a single organic composition present in the aerosol.

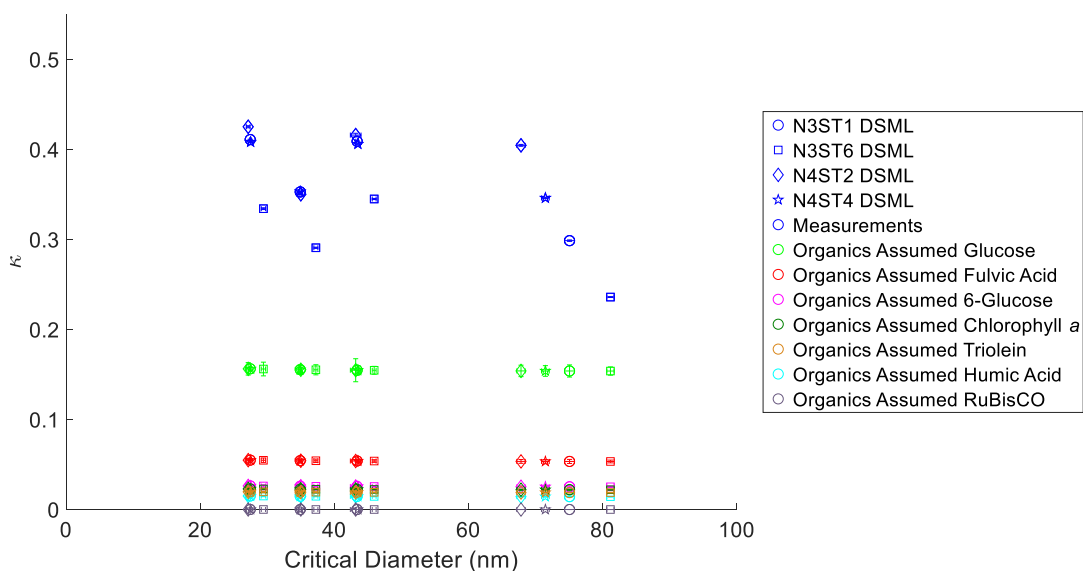


Figure 20. Measured and predicted κ values for DSML samples, assuming DSML samples contain no salts.

κ values from desalinated microlayer samples do not include the small amount of salt remaining after dialysis. The empty shapes correlate to the desalinated sea surface microlayer samples and the different shapes represent the different stations where the samples were collected. The dark blue markers indicate the κ values calculated from direct CCN measurements. The other colored markers are for a predicted κ value assuming a single organic composition present in the aerosol.

From the κ values predicted for the DSML samples shown in Figure 20, it was evident that some of the organic compositions used were more accurate to predicting a κ value close to the κ values from CCN measurements. From this figure it appeared that glucose was the most representative organic composition when trying to predict a κ value close to the DSML κ value. The trend for the predicted κ values for the DSML samples show that with an increasing number of carbon atoms in the organic molecule the κ values decrease. Glucose had the fewest number of carbon atoms and RuBisCO had the highest number of carbon atoms in the organic compositions selected. However, there was still a gap between the predicted κ values from the DSML samples and the calculated κ values from the CCN measurements. While the reduction of salts from the desalination process was significant, the ion chromatography data measured there was still salt

present in the DSML samples. To close the gap between the predictions and the measurements of the DSML κ values, salt was added to the composition in the DSML samples according to the ion chromatography data. In this case the DSML samples were no longer considered organics only. The DSML κ predictions were treated like a mixture of inorganics and organics like the SML κ predictions but the amount of salt in the DSML mixtures was significantly lower than the SML mixtures. Even though the desalination process was effective the ratio of salts to organics remaining in the DSML samples was $99.1\% \pm 0.30\%$ salts and $0.89\% \pm 0.30\%$ for organics. Figure 21 shows how the DSML κ predictions changed with the addition of salts. The organic compositions that previously appeared to be the most representative are now far from matching the DSML κ values from measurements. This again showed how large of an influence the salt had in affecting the κ values. From this adjustment the most representative organic composition to predict a κ value close to the measured DSML κ value is RuBisCO. Fundamentally, this organic composition is a more logical choice because of the desalination process. It was expected that the desalination process would remove the salts in the sample but also remove some of the smaller organics, such as glucose. RuBisCO is a large enough molecule that it should have staying within the sample during desalination. For the SML samples the organic composition that provided the best κ values compared to the κ values from the CCN measurements could not be determined. There was not a significant difference in the κ values predicted for the SML samples with the different organic compositions used.

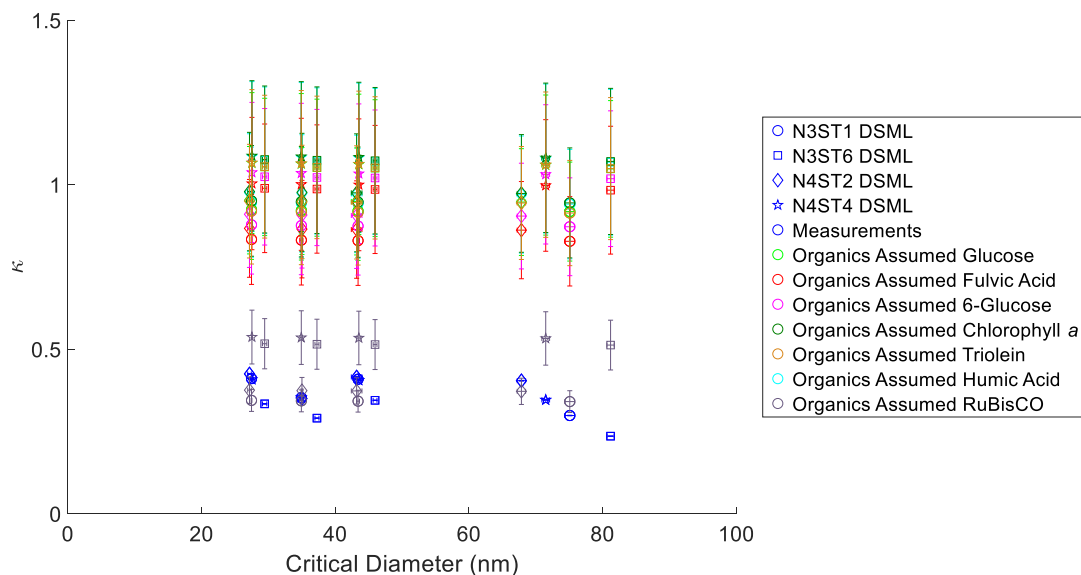


Figure 21. Varying the organic composition, assuming DSML samples contain salts using ion chromatography data

κ values from desalinated microlayer samples do include the small amount of salt remaining after dialysis. The empty shapes correlate to the desalinated sea surface microlayer samples and the different shapes represent the different stations where the samples were collected. The dark blue markers indicate the κ values calculated from direct CCN measurements. The other colored markers are for a predicted κ value assuming a single organic composition present in the aerosol.

4.3. Interpreting Ambient CCN Aerosol Cruise Data

From analyzing the aerosols generated by the SML and DSML samples, the most representative organic composition of RuBisCO can be utilized in predicting κ values for the ambient CCN aerosol from the NAAMES 3 and NAAMES 4 field campaigns. There was a noticeable difference in the aerosols ability to activate as CCN between NAAMES 3 and NAAMES 4. During the NAAMES 3 field campaign the concentration of aerosols able to activate as CCN at a given supersaturation was consistent across stations at the same supersaturation. During the NAAMES 4 campaign there was a decrease in the number of aerosols able to activate as CCN at a given supersaturation and then an increase in the number of aerosols able to activate as CCN at a given supersaturation. Figure 22 and Figure 23 show the ambient CCN aerosol data collected

during NAAMES 3 and NAAMES 4 respectively. Since RuBisCO was the most representative organic composition when predicting κ values for the SML, predictions could be made for the ambient CCN aerosols κ values using this same organic composition. Is the use of RuBisCO as the organic composition also representative of the organics present in the aerosol measurements?

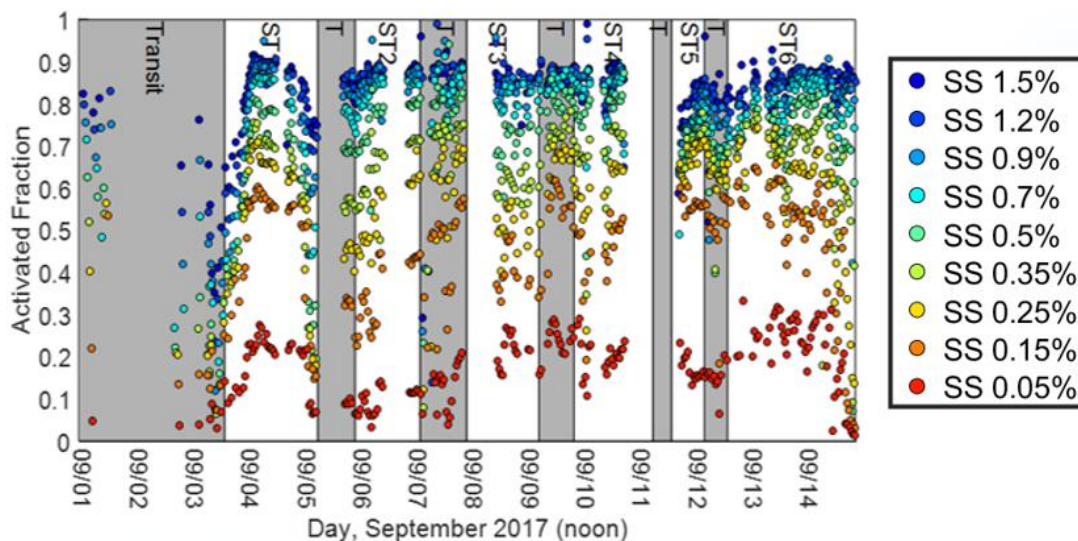


Figure 22. NAAMES 3 ambient CCN aerosol data

Grey bars indicate the times where the ship was in transit and the white bars indicate where the ship was stationary at a sampling station.

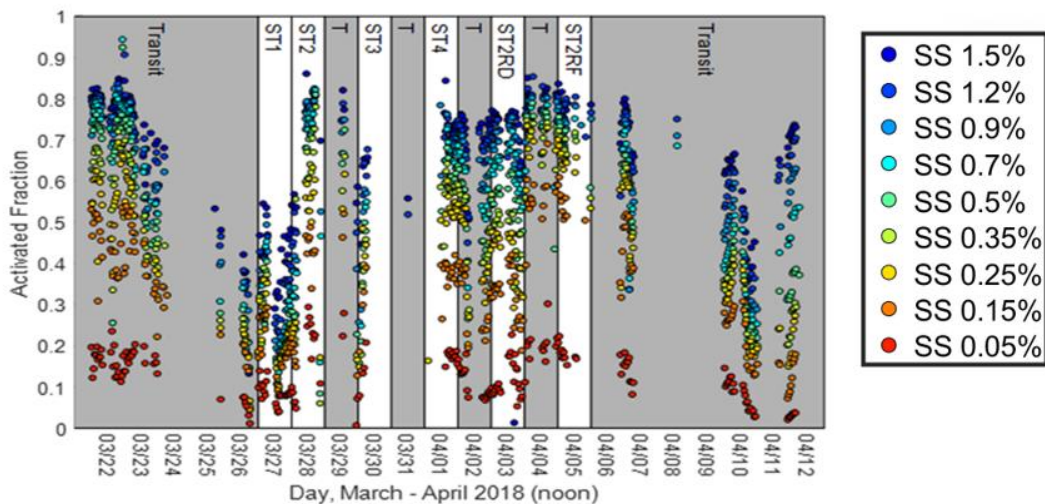


Figure 23. NAAMES 4 ambient CCN aerosol data

Grey bars indicate the times where the ship was in transit and the white bars indicate where the ship was stationary at a sampling station.

4.3.1. Variation in κ and Critical Diameter by Station for Ambient CCN Aerosols

Figure 24 shows the variation in the critical diameter for the ambient CCN aerosols by station.

The critical diameters calculated for the two stations from NAAMES 3 had smaller diameters than the critical diameters calculated for the two stations from NAAMES 4. The microlayer samples selected for this analysis were from the highest and lowest chlorophyll *a* stations from each cruise. In the figure below the two stations that were sampled during the lowest chlorophyll *a* concentrations (N3ST1 and N4ST4) had the smaller critical diameters than the two stations sampled during the highest chlorophyll *a* concentrations (N3ST6 and N4ST2).

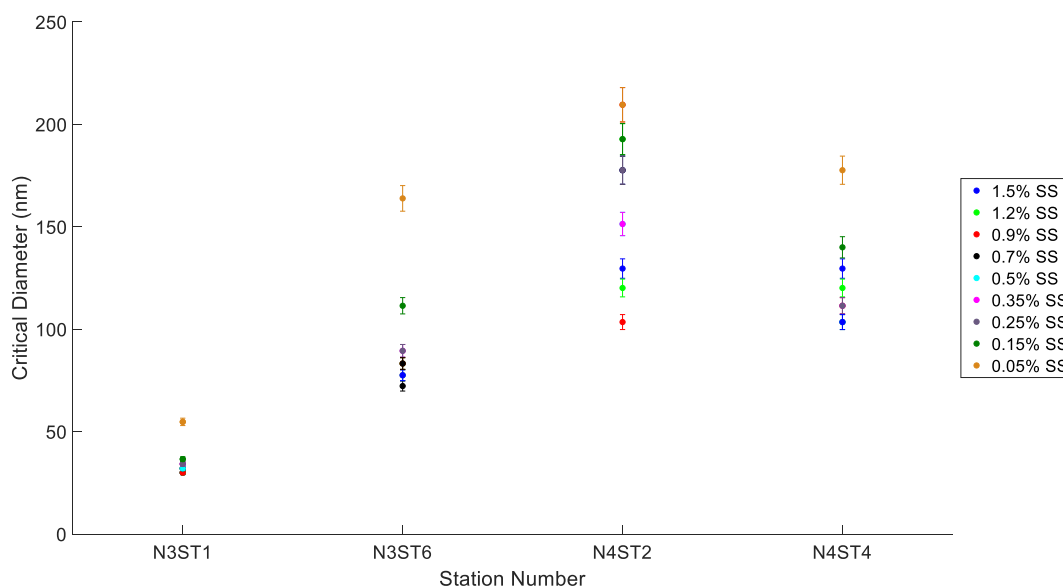


Figure 24. Critical diameters by station for ambient CCN aerosol measurements
 Each color represents aerosols measurements taken at a different supersaturation.

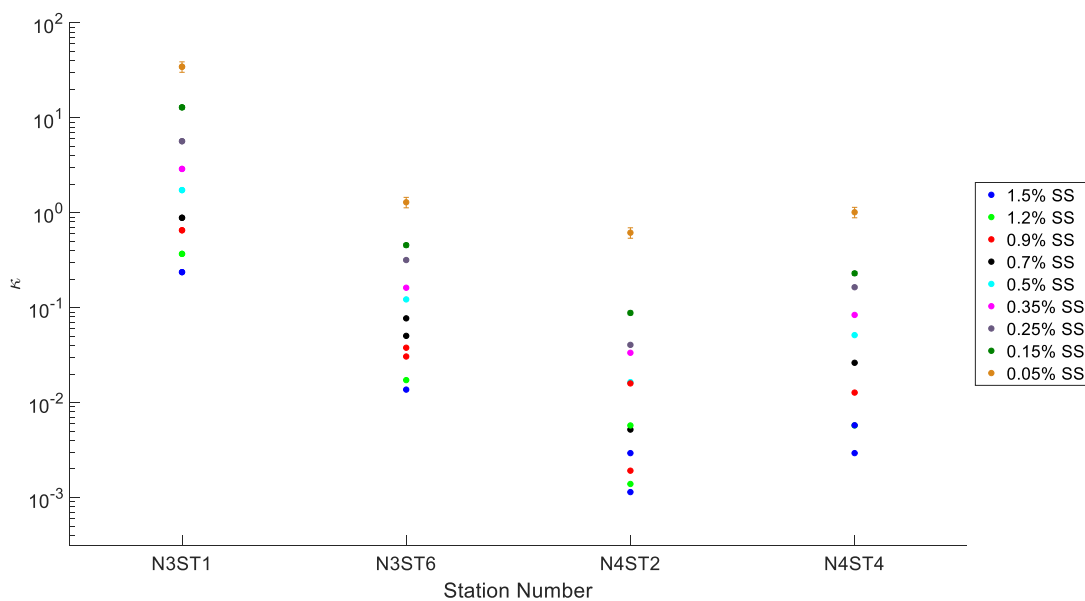


Figure 25. κ by station for ambient CCN aerosol measurements
 Each color represents aerosols measurements taken at a different supersaturation. Due to several outliers in the κ values for N3ST1, the y-axis has been changed to log scale to better display the variation in the data.

From comparing Figure 24 and Figure 25 to the critical diameter and κ values by station for the SML and DSML samples, Figure 15 and Figure 16, variations can be seen in the data. It appears that there is a difference between the critical diameters of the ambient aerosol CCN data and the aerosols generated by the SML and DSML samples.

4.3.2. Ambient CCN Aerosol κ Results

After calculating the κ values for the ambient CCN aerosols, the organic composition that was considered the most representative for the microlayer samples was utilized in predicting κ values for the ambient CCN aerosols. Since the exact ratio of inorganics to organics within the aerosol is unknown, an upper bound κ and lower bound κ were determined. In the lower κ bound the entire aerosol composition is assumed to be only organic, specifically RuBisCO. In the upper κ bound the aerosol composition is considered to be the same ratio of inorganics to organics as in the SML samples. The lower bound κ should be representative of an overly conservative amount of organics present in the aerosol while the upper bound κ should be representative of an overly conservative amount of salt present in the aerosol. Figure 26 and Figure 27 show how accurate these assumptions of chemical composition were compared to the values of κ from the ambient CCN aerosols.

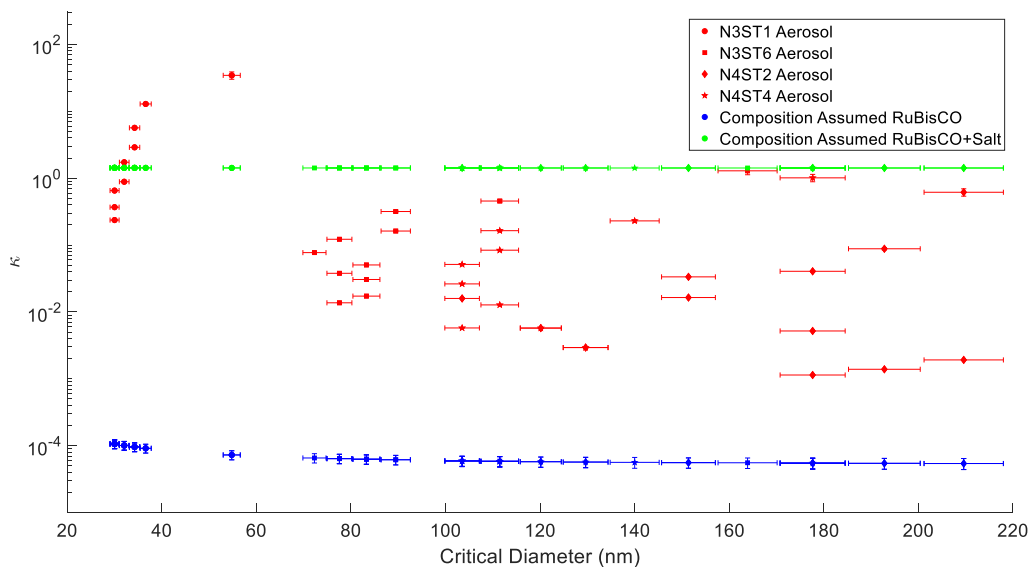


Figure 26. Varying composition data in ambient CCN aerosol κ measurements

Due to several outliers in the κ values for N3ST1, the y-axis has been changed to log scale to better display the variation in the data.

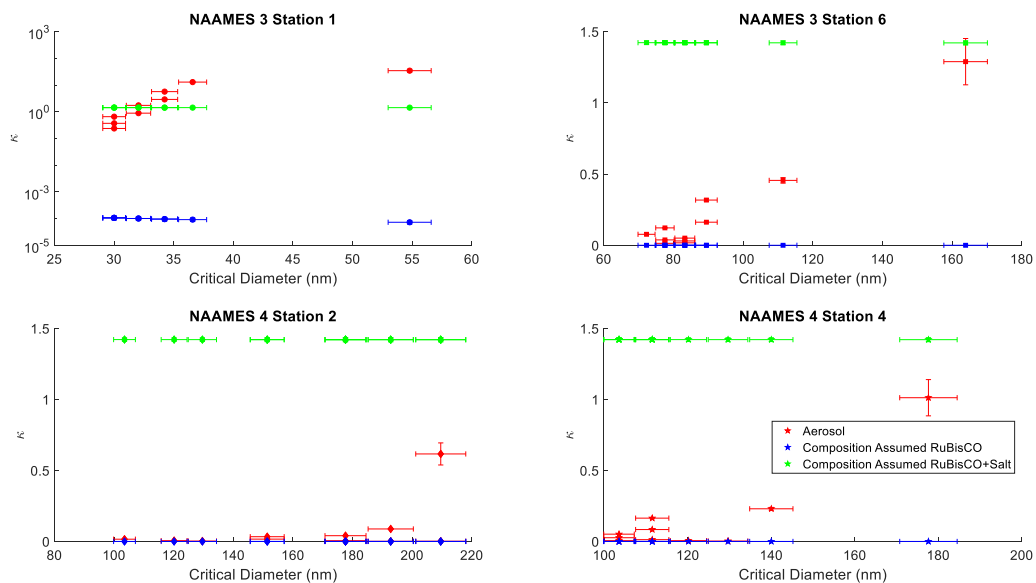


Figure 27. Varying composition data in ambient CCN aerosol κ measurements displayed by station

Due to several outliers in the κ values for N3ST1, the y-axis has been changed to log scale to better display the variation in the data in the first subplot for N3ST1.

In general, the measured ambient CCN aerosol κ values fell between the upper and lower bounds of κ . This was expected as the chemical composition data to set each bound was overly conservative. The predicted κ values for the ambient CCN aerosol appeared closer to the κ values for the composition of pure of RuBisCO. The κ of pure RuBisCO was calculated to be 5.16×10^{-5} and the κ for the mixture of RuBisCO and salts in artificial seawater was calculated to be 1.28 ± 0.004 . The κ values calculated for the ambient CCN aerosols was 6.6 ± 11.2 , 0.23 ± 0.38 , 0.07 ± 0.17 , and 0.16 ± 0.31 for N3ST1, N3ST6, N4ST2, and N4ST4 respectively. Based on these statistics the ambient CCN aerosol κ values were not as close to the pure RuBisCO κ values as they appear. These κ values calculated for the ambient CCN aerosols are in between the two different composition scenarios considered.

5. DISCUSSION

Salt driving CCN activity in a marine environment is often assumed to be true but rarely quantified with experimental data. By comparing the CCN activity of SML samples to the CCN activity of DSML samples the influence of salts on marine aerosol hygroscopicity was measured. Desalinating the SML samples reduced the κ values calculated using the CCN measurements by $62.5\% \pm 15.6\%$. This experiment quantified the impacts that salts have on the marine aerosol population to form clouds.

The κ values calculated from the CCN measurements for the SML samples ranged 0.96 ± 0.12 . The κ values calculated using the CCN measurements for the DSML samples were 0.36 ± 0.05 . These values are similar to marine κ values measured by Collins et al. (2016), from these data the marine κ values ranged from 0.7 to 1.4 with an average of 0.95 ± 0.15 (Collins et al., 2016). The κ values calculated from aerosols generated by the SML and DSML samples were higher than the κ values measured in a field study along the coast of Southern California, this study had a campaign average of 0.22 ± 0.12 (Gaston et al., 2018). This field project did report that there was possible influence from pollution and anthropogenic sources which could decrease the κ values. The SML and DSML κ values were also similar to κ values measured in remote marine regions of the South China Sea/East Sea. In this study they found average κ values of 0.40 for samples dominated by aged accumulation mode smoke; 0.65 for accumulation mode marine aerosol; 0.60 in an anthropogenic aerosol plume; and 0.22 during a short period with elevated levels of volatile organic compounds (Atwood et al., 2017). The κ values from the SML samples

were in good agreement with the global mean κ for marine regions of 0.72 ± 0.24 (Pringle et al., 2010).

A way to improve the composition information for the ambient CCN aerosol population would be to measure the concentration of inorganics to organics present in the aerosols. Then the predicted κ values could be adjusted to more accurately describe the ambient CCN aerosol population. While this may provide some insight into the organics present in the ambient CCN aerosol measurements, there are clearly other factors to consider that prevent these ambient CCN aerosol κ predictions from being comparable to the predicted and measured κ values from the microlayer samples. There were differences between the aerosols generated in the laboratory to create the SML and DSML aerosols compared to the ambient aerosols measured. While the nebulizer in the laboratory is useful for creating a model system, it does not produce the same size distribution being generated naturally. This explains differences in the aerosol size and supersaturation needed to activate as CCN between the ambient aerosol and the aerosols generated by the SML and DSML samples. There are also other meteorological parameters that would cause differences in the ambient aerosols and the aerosols generated in the laboratory. These factors could include wind speed, wave breaking, transport of different aerosol population, and chemical reactions of the aerosols. The storage of the SML and DSML samples could have caused changes to the composition in the samples. Freezing the samples and performing the desalination process could have increased cell lysis within the samples. This would have altered the sample composition in a way that affected the aerosols being generated from those samples. These same changes would not be reflected in the ambient aerosol population.

When predicting κ values for the ambient CCN aerosol, there are considerations to include other than the most representative organic composition of RuBisCO determined from the predictions of κ values for the DSML samples. Fundamentally, it was expected that the aerosols being produced from the SML and DSML samples would be different from the aerosols being measured by the ambient data. The SML and DSML aerosols may be a part of the population of aerosols being measured by the ambient CCN aerosol but would not compose the entire ambient CCN aerosol population. There could be other processes that change the ambient aerosol composition or an influx of aerosols from sources other than the microlayer. It is difficult to extrapolate the data from the SML and DSML aerosols to apply this information to the ambient aerosols.

6. CONCLUSION

The predicted κ values for the aerosols generated by the SML samples were largely driven by the concentration of salts present in the aerosols. In these aerosols the organics provided little influence over the κ values. The predicted κ across the different organic compositions for the SML samples was 1.28 ± 0.004 . The κ values calculated from the CCN measurements for the SML samples ranged 0.96 ± 0.12 . By adjusting the organic composition when predicting κ values for the aerosols generated by the DSML samples, the κ predictions were influenced by the varied organic compositions. The most representative organic composition when predicting the κ values from the DSML samples was RuBisCO. RuBisCO predicted κ values of 0.44 ± 0.087 . These values were comparable to the κ values calculated for the DSML samples using the CCN measurements which ranged 0.36 ± 0.05 . In these aerosols the influence of the organics on calculating κ values was more apparent. Even in the DSML samples, which had a reduced salt concentration of at least 95.95%, the amount of salt remaining after the desalination process was able to strongly influence the κ values for the aerosols generated by the DSML samples.

For the predicted κ values from the DSML samples, the most representative organic composition was RuBisCO. Due to the size of RuBisCO, it was assumed that RuBisCO would remain in the samples during the desalination process. Also, from the amino acid analysis the SML samples contained more labile organics than the subsurface waters. The labile organics are generally larger in size due to the fact they are less diagenetically altered. These organics would not have been affected by the desalination process. This information reinforces choosing an organic as large as RuBisCO as an organic composition when predicting κ values. The high abundance of

RuBisCO in the ocean is another justification for using it as the composition for the organics in the microlayer samples.

For the ambient CCN aerosol measurements, it was unclear how representative using the organic composition of RuBisCO was in predicting the κ values. If there was RuBisCO located in the SML, it is conceivable that these organics could be lofted into the ambient CCN aerosol population depending on the wind speed and wave breaking. Without knowing more about the organic to inorganic ratio in the ambient CCN aerosols, the best κ predictions are to represent a higher bound value for κ and a lower bound value for κ . If additional information were known about the ratio of inorganics to organics in the ambient CCN aerosols, then the κ predictions for the ambient CCN aerosols could determine if the aerosols originated from the SML were being lofted into the atmosphere. If these κ predictions were not well matched to the calculated κ values for the ambient CCN aerosol data this could mean that the aerosols are being lofted into the atmosphere but there are other factors to consider.

REFERENCES

- Amon, R. M. W., & Benner, R. (1996). Bacterial utilization of different size classes of dissolved organic matter. *Limnology and Oceanography*, *41*(1), 41-51. doi:10.4319/lo.1996.41.1.0041
- Amon, R. M. W., Fitznar, H. P., & Benner, R. (2001). Linkages among the bioreactivity, chemical composition, and diagenetic state of marine dissolved organic matter. *Limnology and Oceanography*, *46*(2), 287-297. doi:10.4319/lo.2001.46.2.0287
- Arts, M. T. (1999). *Lipids in freshwater ecosystems*. Springer, New York: Oxford.
- Atwood, S. A., Reid, J. S., Kreidenweis, S. M., Blake, D. R., Jonsson, H. H., Lagrosas, N. D., . . . Simpas, J. B. (2017). Size-resolved aerosol and cloud condensation nuclei (CCN) properties in the remote marine South China Sea - Part 1: Observations and source classification. *Atmospheric Chemistry and Physics*, *17*(2), 1105-1123. doi:10.5194/acp-17-1105-2017
- Bates, T. S., Quinn, P. K., Frossard, A. A., Russell, L. M., Hakala, J., Petaja, T., . . . Keene, W. C. (2012). Measurements of ocean derived aerosol off the coast of California. *Journal of Geophysical Research-Atmospheres*, *117*, 13. doi:10.1029/2012jd017588
- Behrenfeld, M. J., Moore, R. H., Hostetler, C. A., Graff, J., Gaube, P., Russell, L. M., . . . Ziemba, L. (2019). The North Atlantic Aerosol and Marine Ecosystem Study (NAAMES): Science Motive and Mission Overview. *Frontiers in Marine Science*, *6*(122). doi:10.3389/fmars.2019.00122
- Bigg, E. K., & Leck, C. (2008). The composition of fragments of bubbles bursting at the ocean surface. *Journal of Geophysical Research-Atmospheres*, *113*(D11), 7. doi:10.1029/2007jd009078
- Brooks, S. D., & Thornton, D. C. O. (2018). Marine Aerosols and Clouds. *Annual Review of Marine Science*, *10*(1), 289-313. doi:10.1146/annurev-marine-121916-063148
- Carslaw, K. S., Lee, L. A., Reddington, C. L., Pringle, K. J., Rap, A., Forster, P. M., . . . Pierce, J. R. (2013). Large contribution of natural aerosols to uncertainty in indirect forcing. *Nature*, *503*(7474), 67-+. doi:10.1038/nature12674
- Chen, Y., Yang, G. P., Xia, Q. Y., & Wu, G. W. (2016). Enrichment and characterization of dissolved organic matter in the surface microlayer and subsurface water of the South Yellow Sea. *Marine Chemistry*, *182*, 1-13. doi:10.1016/j.marchem.2016.04.001

- Choi, J. H., Jang, E., Yoon, Y. J., Park, J. Y., Kim, T.-W., Becagli, S., . . . Jang, K. S. Influence of biogenic organics on the chemical composition of Arctic aerosols. *Global Biogeochemical Cycles*, 0(ja). doi:10.1029/2019gb006226
- Cochran, R. E., Laskina, O., Trueblood, J. V., Estillore, A. D., Morris, H. S., Jayarathne, T., . . . Grassian, V. H. (2017). Molecular Diversity of Sea Spray Aerosol Particles: Impact of Ocean Biology on Particle Composition and Hygroscopicity. *Chem*, 2(5), 655-667. doi:10.1016/j.chempr.2017.03.007
- Collins, D. B., Bertram, T. H., Sultana, C. M., Lee, C., Axson, J. L., & Prather, K. A. (2016). Phytoplankton blooms weakly influence the cloud forming ability of sea spray aerosol. *Geophysical Research Letters*, 43(18), 9975-9983. doi:10.1002/2016gl069922
- Cowie, G. L., & Hedges, J. I. (1994). BIOCHEMICAL INDICATORS OF DIAGENETIC ALTERATION IN NATURAL ORGANIC-MATTER MIXTURES. *Nature*, 369(6478), 304-307. doi:10.1038/369304a0
- Davis, J., & Benner, R. (2007). Quantitative estimates of labile and semi-labile dissolved organic carbon in the western Arctic Ocean: A molecular approach. *Limnology and Oceanography*, 52(6), 2434-2444. doi:10.4319/lo.2007.52.6.2434
- Davis, J., Kaiser, K., & Benner, R. (2009). Amino acid and amino sugar yields and compositions as indicators of dissolved organic matter diagenesis. *Organic Geochemistry*, 40(3), 343-352. doi:10.1016/j.orggeochem.2008.12.003
- Drozdowska, V., Wrobel, I., Markuszewski, P., Makuch, P., Raczowska, A., & Kowalczyk, P. (2017). Study on organic matter fractions in the surface microlayer in the Baltic Sea by spectrophotometric and spectrofluorometric methods. *Ocean Science*, 13(5), 633-647. doi:10.5194/os-13-633-2017
- Duce, R. A., Mohnen, V. A., Zimmerman, P. R., Grosjean, D., Cautreels, W., Chatfield, R., . . . Wallace, G. T. (1983). ORGANIC MATERIAL IN THE GLOBAL TROPOSPHERE. *Reviews of Geophysics*, 21(4), 921-952. doi:10.1029/RG021i004p00921
- Ellis, R. J. (1979). MOST ABUNDANT PROTEIN IN THE WORLD. *Trends in Biochemical Sciences*, 4(11), 241-244. doi:10.1016/0968-0004(79)90212-3
- Engel, A., Bange, H. W., Cunliffe, M., Burrows, S. M., Friedrichs, G., Galgani, L., . . . Zäncker, B. (2017). The Ocean's Vital Skin: Toward an Integrated Understanding of the Sea Surface Microlayer. *Frontiers in Marine Science*, 4(165). doi:10.3389/fmars.2017.00165
- Engel, A., & Galgani, L. (2016). The organic sea-surface microlayer in the upwelling region off the coast of Peru and potential implications for air-sea exchange processes. *Biogeosciences*, 13(4), 989-1007. doi:10.5194/bg-13-989-2016

- Garrett, W. D. (1965). Collection of Slick-Forming Materials from the Sea Surface. *Limnology and Oceanography*, 10(4), 602-605. doi:10.4319/lo.1965.10.4.0602
- Gaston, C. J., Cahill, J. F., Collins, D. B., Suski, K. J., Ge, J. Y., Barkley, A. E., & Prather, K. A. (2018). The Cloud Nucleating Properties and Mixing State of Marine Aerosols Sampled along the Southern California Coast. *Atmosphere*, 9(2), 16. doi:10.3390/atmos9020052
- Gras, J. L., & Keywood, M. (2017). Cloud condensation nuclei over the Southern Ocean: wind dependence and seasonal cycles. *Atmospheric Chemistry and Physics*, 17(7), 4419-4432. doi:10.5194/acp-17-4419-2017
- Gross, S., Freudenthaler, V., Schepanski, K., Toledano, C., Schafler, A., Ansmann, A., & Weinzierl, B. (2015). Optical properties of long-range transported Saharan dust over Barbados as measured by dual-wavelength depolarization Raman lidar measurements. *Atmospheric Chemistry and Physics*, 15(19), 11067-11080. doi:10.5194/acp-15-11067-2015
- Hudson, J. G., Garrett, T. J., Hobbs, P. V., Strader, S. R., Xie, Y. H., & Yum, S. S. (2000). Cloud condensation nuclei and ship tracks. *Journal of the Atmospheric Sciences*, 57(16), 2696-2706. doi:10.1175/1520-0469(2000)057<2696:ccnast>2.0.co;2
- IPCC. (2014). *IPCC, 2014: Climate Change 2014: Synthesis Report. Contribution of Working Groups I, II and III to the Fifth Assessment Report of the Intergovernmental Panel on Climate Change*. Retrieved from Geneva, Switzerland:
- Kang, M. J., Fu, P. Q., Kawamura, K., Yang, F., Zhang, H. L., Zang, Z. C., . . . Wang, Z. F. (2018). Characterization of biogenic primary and secondary organic aerosols in the marine atmosphere over the East China Sea. *Atmospheric Chemistry and Physics*, 18(19), 13947-13967. doi:10.5194/acp-18-13947-2018
- Köhler, H. (1936). The nucleus in and the growth of hygroscopic droplets. *Transactions of the Faraday Society*, 32(0), 1152-1161. doi:10.1039/TF9363201152
- Kristensen, T. B., Müller, T., Kandler, K., Benker, N., Hartmann, M., Prospero, J. M., . . . Stratmann, F. (2016). Properties of cloud condensation nuclei (CCN) in the trade wind marine boundary layer of the western North Atlantic. *Atmospheric Chemistry and Physics*, 16(4), 2675-2688. doi:10.5194/acp-16-2675-2016
- Kuznetsova, M., & Lee, C. (2002). Dissolved free and combined amino acids in nearshore seawater, sea surface microlayers and foams: Influence of extracellular hydrolysis. *Aquatic Sciences*, 64(3), 252-268. doi:10.1007/s00027-002-8070-0
- Kuznetsova, M., Lee, C., & Aller, J. (2005). Characterization of the proteinaceous matter in marine aerosols. *Marine Chemistry*, 96(3-4), 359-377. doi:10.1016/j.marchem.2005.03.007

- Meskhidze, N., & Nenes, A. (2007). Phytoplankton and cloudiness in the Southern Ocean (vol 314, pg 1419, 2006). *Science*, 317(5834), 43-43.
- Modini, R. L., Russell, L. M., Deane, G. B., & Stokes, M. D. (2013). Effect of soluble surfactant on bubble persistence and bubble-produced aerosol particles. *Journal of Geophysical Research-Atmospheres*, 118(3), 1388-1400. doi:10.1002/jgrd.50186
- Moore, M. J. K., Furutani, H., Roberts, G. C., Moffet, R. C., Gilles, M. K., Palenik, B., & Prather, K. A. (2011). Effect of organic compounds on cloud condensation nuclei (CCN) activity of sea spray aerosol produced by bubble bursting. *Atmospheric Environment*, 45(39), 7462-7469. doi:10.1016/j.atmosenv.2011.04.034
- Moore, R. H., Bahreini, R., Brock, C. A., Froyd, K. D., Cozic, J., Holloway, J. S., . . . Nenes, A. (2011). Hygroscopicity and composition of Alaskan Arctic CCN during April 2008. *Atmospheric Chemistry and Physics*, 11(22), 11807-11825. doi:10.5194/acp-11-11807-2011
- Moore, R. H., Cerully, K., Bahreini, R., Brock, C. A., Middlebrook, A. M., & Nenes, A. (2012). Hygroscopicity and composition of California CCN during summer 2010. *Journal of Geophysical Research-Atmospheres*, 117, 14. doi:10.1029/2011jd017352
- Moore, R. H., Ingall, E. D., Sorooshian, A., & Nenes, A. (2008). Molar mass, surface tension, and droplet growth kinetics of marine organics from measurements of CCN activity. *Geophysical Research Letters*, 35(7), 5. doi:10.1029/2008gl033350
- North, G. R., & Erukhimova, T. L. (2009). *Atmospheric thermodynamics : elementary physics and chemistry*. Cambridge, UK ;: Cambridge University Press.
- O'Dowd, C. D., Facchini, M. C., Cavalli, F., Ceburnis, D., Mircea, M., Decesari, S., . . . Putaud, J. P. (2004). Biogenically driven organic contribution to marine aerosol. *Nature*, 431(7009), 676-680. doi:10.1038/nature02959
- Orellana, M. V., & Hansell, D. A. (2012). Ribulose-1,5-bisphosphate carboxylase/oxygenase (RuBisCO): A long-lived protein in the deep ocean. *Limnology and Oceanography*, 57(3), 826-834. doi:10.4319/lo.2012.57.3.0826
- Ovadnevaite, J., Ceburnis, D., Martucci, G., Bialek, J., Monahan, C., Rinaldi, M., . . . O'Dowd, C. (2011). Primary marine organic aerosol: A dichotomy of low hygroscopicity and high CCN activity. *Geophysical Research Letters*, 38, 5. doi:10.1029/2011gl048869
- Petters, M. D., & Kreidenweis, S. M. (2007). A single parameter representation of hygroscopic growth and cloud condensation nucleus activity. *Atmospheric Chemistry and Physics*, 7(8), 1961-1971. doi:10.5194/acp-7-1961-2007

- Petters, M. D., & Kreidenweis, S. M. (2013). A single parameter representation of hygroscopic growth and cloud condensation nucleus activity - Part 3: Including surfactant partitioning. *Atmospheric Chemistry and Physics*, *13*(2), 1081-1091. doi:10.5194/acp-13-1081-2013
- Phillips, B. N., Royalty, T. M., Dawson, K. W., Reed, R., Petters, M. D., & Meskhidze, N. (2018). Hygroscopicity- and Size-Resolved Measurements of Submicron Aerosol on the East Coast of the United States. *Journal of Geophysical Research-Atmospheres*, *123*(3), 1826-1839. doi:10.1002/2017jd027702
- Pringle, K. J., Tost, H., Pozzer, A., Poschl, U., & Lelieveld, J. (2010). Global distribution of the effective aerosol hygroscopicity parameter for CCN activation. *Atmospheric Chemistry and Physics*, *10*(12), 5241-5255. doi:10.5194/acp-10-5241-2010
- Quinn, P. K., Bates, T. S., Schulz, K. S., Coffman, D. J., Frossard, A. A., Russell, L. M., . . . Kieber, D. J. (2014). Contribution of sea surface carbon pool to organic matter enrichment in sea spray aerosol. *Nature Geoscience*, *7*(3), 228-232. doi:10.1038/ngeo2092
- Reinthal, T., Sintes, E., & Herndl, G. J. (2008). Dissolved organic matter and bacterial production and respiration in the sea-surface microlayer of the open Atlantic and the western Mediterranean Sea. *Limnology and Oceanography*, *53*(1), 122-136. doi:10.4319/lo.2008.53.1.0122
- Rinaldi, M., Fuzzi, S., Decesari, S., Marullo, S., Santolero, R., Provenzale, A., . . . Facchini, M. C. (2013). Is chlorophyll-a the best surrogate for organic matter enrichment in submicron primary marine aerosol? *Journal of Geophysical Research-Atmospheres*, *118*(10), 4964-4973. doi:10.1002/jgrd.50417
- Russell, L. M., Hawkins, L. N., Frossard, A. A., Quinn, P. K., & Bates, T. S. (2010). Carbohydrate-like composition of submicron atmospheric particles and their production from ocean bubble bursting. *Proceedings of the National Academy of Sciences of the United States of America*, *107*(15), 6652-6657. doi:10.1073/pnas.0908905107
- Sellegrri, K., O'Dowd, C. D., Yoon, Y. J., Jennings, S. G., & de Leeuw, G. (2006). Surfactants and submicron sea spray generation. *Journal of Geophysical Research-Atmospheres*, *111*(D22), 12. doi:10.1029/2005jd006658
- Taylor, J. W., Choulaton, T. W., Blyth, A. M., Flynn, M. J., Williams, P. I., Young, G., . . . Rosenberg, P. D. (2016). Aerosol measurements during COPE: composition, size, and sources of CCN and INPs at the interface between marine and terrestrial influences. *Atmospheric Chemistry and Physics*, *16*(18), 11687-11709. doi:10.5194/acp-16-11687-2016

- Thornton, D. C. O. (2018). Coomassie Stainable Particles (CSP): Protein Containing Exopolymer Particles in the Ocean. *Frontiers in Marine Science*, 5, 10. doi:10.3389/fmars.2018.00206
- Thornton, D. C. O., Brooks, S. D., & Chen, J. (2016). Protein and Carbohydrate Exopolymer Particles in the Sea Surface Microlayer (SML). *Frontiers in Marine Science*, 3, 14. doi:10.3389/fmars.2016.00135
- Wurl, O., & Holmes, M. (2008). The gelatinous nature of the sea-surface microlayer. *Marine Chemistry*, 110(1-2), 89-97. doi:10.1016/j.marchem.2008.02.009
- Zäncker, B., Bracher, A., Röttgers, R., & Engel, A. (2017). Variations of the Organic Matter Composition in the Sea Surface Microlayer: A Comparison between Open Ocean, Coastal, and Upwelling Sites Off the Peruvian Coast. *Frontiers in Microbiology*, 8(2369). doi:10.3389/fmicb.2017.02369
- Zieger, P., Vaisanen, O., Corbin, J. C., Partridge, D. G., Bastelberger, S., Mousavi-Fard, M., . . . Salter, M. E. (2017). Revising the hygroscopicity of inorganic sea salt particles. *Nature Communications*, 8, 10. doi:10.1038/ncomms15883

APPENDIX A

DIALYSIS TUBING SPECIFICATIONS AND STEPS FOR DESALINATION

Dialysis tubing specifications:

- Spectrum Labs, 7 Spectra/Pore Dialysis Membrane
- Molecular Weight Cut-Off (MWCO): 1,000 Daltons
- Wet in: 0.1% sodium azide
- Flat Width: 38 mm
- Diameter: 24 mm
- Volume/Length: 4.6 ml/cm

Steps for desalinating samples:

1. Unrolled dialysis tubing and measured out 6.6 cm (held 10 ml and allowed enough space to clamp the ends closed)
2. Rinsed dialysis tubing with ultra-high purity (UHP) water inside and outside
3. Clamped one side of the tubing closed
4. Filled dialysis tubing with 10 ml of sample
5. Clamped other side of tubing
6. Placed in a tub filled with UHP water
7. Stirred tub of water to assist in desalination process every two hours (three times)
8. Checked salinity after 6 hours of desalination using a portable refractometer
9. Changed water in the tub, again using UHP water
10. Rechecked salinity of the samples after 24 hours of dialysis
11. Poured samples out of the dialysis tubing and stored inside cleaned test tubes

APPENDIX B

SIGMAPLOT REPORT RESULTS

One Way Analysis of Variance

Friday, October 18, 2019, 4:30:58 PM

Data source: Data 1 in Notebook 1

Normality Test (Shapiro-Wilk): Failed ($P < 0.050$)

Test execution ended by user request, ANOVA on Ranks begun

Kruskal-Wallis One Way Analysis of Variance on Ranks

Friday, October 18, 2019, 4:30:58 PM

Data source: Data 1 in Notebook 1

Group	N	Missing	Median	25%	75%
blank	7	0	71.280	70.830	73.970
SML	21	0	69.900	69.570	70.395
DSML	16	0	71.150	68.612	72.070

H = 15.574 with 2 degrees of freedom. ($P = < 0.001$)

The differences in the median values among the treatment groups are greater than would be expected by chance; there is a statistically significant difference ($P = < 0.001$)

To isolate the group or groups that differ from the others use a multiple comparison procedure.

All Pairwise Multiple Comparison Procedures (Dunn's Method) :

Comparison	Diff of Ranks	Q	P<0.05
blank vs SML	20.405	3.640	Yes
blank vs DSML	9.165	1.575	No
DSML vs SML	11.240	2.637	Yes

Note: The multiple comparisons on ranks do not include an adjustment for ties.

APPENDIX C

ARCHIVED DATA FOR NAAMES 1-4

To access the NAAMES archived data for each field campaign, the links below can be used.

NAAMES 1 (November 2015):

<https://www-air.larc.nasa.gov/cgi-bin/ArcView/naames.2015?ATLANTIS=1>

NAAMES 2 (May 2016):

<https://www-air.larc.nasa.gov/cgi-bin/ArcView/naames.2016?ATLANTIS=1>

NAAMES 3 (August-September 2017):

<https://www-air.larc.nasa.gov/cgi-bin/ArcView/naames.2017?ATLANTIS=1>

NAAMES 4 (March-April 2018):

<https://www-air.larc.nasa.gov/cgi-bin/ArcView/naames.2018?ATLANTIS=1>

APPENDIX D

NAAMES HEADER FILE FOR NAAMES 3 CCN DATA

51, 1001

Brooks, SarahD

Texas A&M University

Differential Mobility Stepping Cloud Condensation Nuclei Counter

NAAMES3

1,1

2017, 09, 01, 2018, 02, 09

0

startUTC, seconds

6

1, 1, 1, 1, 1, 1

-9999, -9999, -9999, -9999, -9999, -9999

stopUTC, seconds

ss, %, supersaturation

nccn, #/ccm, ccnumberconcentration

lat, degrees, latitude

lon, degrees, longitude

alt, meters, altitude

10

During NAAMES 3, Cloud Condensation Nuclei Measurements were conducted continuously in one of two modes, either in size resolved sampling mode (naames-

SRCCN_ATLANTIS_201709XX.ict) or ambient sampling mode; ambient data is reported in this file.

Uncertainties in supersaturation measurements reported are based on pre- and post-cruise calibrations performed following methods employed in our previous work, Deng, 2014 based on Rose, 2008.

Periods with no data record due to operational difficulty and maintenance have been removed.

When the instrument changed supersaturation from low to high, a thermal equilibration time of 2 minutes was removed. When the instrument changed from high to low supersaturation, a thermal equilibration time of 5 minutes was removed.

The height of the aerosol inlet is 17 meters above the water line on flat water.

Relative wind was calculated using ship speed, ship direction and, windspeed. Data that was sampled with a relative wind that blew from the rear of the ship (90 to 270 degrees), which may have been influenced by ship emissions was removed from the data.

Latitude and longitude are recorded from the R/V Atlantis's navigational system (Switched Source CNAV 3050), which is reported in 15 minute increments and stored on the ship's intranet.

If there are any remaining questions, please contact the PI, Dr. Sarah Brooks.

Rose et. al. Calibration and Measurement Uncertainties of a Continuous-Flow Cloud

Condensation Nuclei Counter (DMT-CCNC): CCN Activation of Ammonium Sulfate and Sodium Chloride Aerosol Particles in Theory and Experiment. *Atmos. Chem. Phys.*, 8, 1153-1179, 2008.

Deng et. al. Using Raman Microspectroscopy to Determine Chemical Composition and Mixing State of Airborne Marine Aerosols over the Pacific Ocean. *Aerosol Science and Technology*, Vol 48, Issue 2, 2014.

21

PI_CONTACT_INFO: 1204 Eller, Atmospheric Sciences, College Station Texas. Email:

sbrooks@tamu.edu

PLATFORM: ATLANTIS

LOCATION: N/A

ASSOCIATED_DATA: See GPS info above

INSTRUMENT_INFO: Cloud Condensation Nuclei Counter (DMT CCN).

DATA_INFO: The data is reported as the mean concentration of aerosol particles in #/ccm in the time window between startUTC and stopUTC, but not including the times when particles had not yet traveled through the DMA column to the instruments.

UNCERTAINTY: Uncertainties in the optical particle counter (OPC) for the CCN of +/- 10% for one standard deviation is based on uncertainties in OPC temperature, volumetric flow rate, particle coincidence rate both in physical space and the data acquisition electronics, and the absolute pressure at the inlet. The standard deviation in supersaturation is reported in the data. The supersaturation uncertainty is estimated conservatively at +/- 0.03%, where variation in the inlet temperature, pressure, and calibration technique prevent a more accurate measurement.

ULOD_FLAG: -7777

ULOD_VALUE: N/A

LLOD_FLAG: -8888

LLOD_VALUE: N/A

DM_CONTACT_INFO: See PI

PROJECT_INFO: NAAMES 2017 Mission

STIPULATIONS_ON_USE: For responsible scientific use of the data sets provided in this archive, data users are strongly encouraged to carefully study the file headers and directly consult with the instrument PIs. Please acknowledge the data source and offer co-authorship to relevant instrument PIs when appropriate.

OTHER_COMMENTS: N/A

REVISION: R0

RA: Initial submission to ICARTT database

RB: Header edited with example filename for size-resolved data

R0: Publication data, no changes from RB

startUTC,stopUTC,ss,nccn,lat,lon,alt

APPENDIX E

NAAMES HEADER FILE FOR NAAMES 4 CCN DATA

48, 1001

Brooks, SarahD

Texas A&M University

Droplet Measurement Technologies Cloud Condensation Nuclei Counter (DMT CCN)

NAAMES4

1,1

2018, 03, 22, 2018, 08, 31

0

startUTC, seconds

6

1, 1, 1, 1, 1, 1

-9999, -9999, -9999, -9999, -9999, -9999

stopUTC, seconds

ss, %, supersaturation

nccn, #/ccm, ccnumberconcentration

lat, degrees, latitude

lon, degrees, longitude

alt, meters, altitude

10

During NAAMES 4, Cloud Condensation Nuclei measurements were conducted continuously in one of two modes, either in size resolved sampling mode (naames-

SRCCN_ATLANTIS_201803XX.ict) or ambient sampling mode; ambient data is reported in this file.

Uncertainties in supersaturation measurements reported are based on pre- and post-cruise calibrations performed following methods employed in our previous work, Deng, 2014 based on Rose, 2008.

Periods with no data record due to operational difficulty and maintenance have been removed.

When the instrument changed supersaturation from low to high, a thermal equilibration time of 2 minutes was removed. When the instrument changed from high to low supersaturation, a thermal equilibration time of 5 minutes was removed.

The height of the aerosol inlet is 17 meters above the water line on flat water.

Relative wind was calculated using ship speed, ship direction and, windspeed. Data that was sampled with a relative wind that blew from the rear of the ship (90 to 270 degrees), which may have been influenced by ship emissions was removed from the data.

Latitude and longitude are recorded from the R/V Atlantis's navigational system (Switched Source CNAV 3050), which is reported in 15 minute increments and stored on the ship's intranet.

If there are any remaining questions, please contact the PI, Dr. Sarah Brooks.

Rose et. al. Calibration and Measurement Uncertainties of a Continuous-Flow Cloud

Condensation Nuclei Counter (DMT-CCNC): CCN Activation of Ammonium Sulfate and Sodium Chloride Aerosol Particles in Theory and Experiment. *Atmos. Chem. Phys.*, 8, 1153-1179, 2008.

Deng et. al. Using Raman Microspectroscopy to Determine Chemical Composition and Mixing State of Airborne Marine Aerosols over the Pacific Ocean. *Aerosol Science and Technology*, Vol 48, Issue 2, 2014.

18

PI_CONTACT_INFO: 1204 Eller, Atmospheric Sciences, College Station Texas. Email:

sbrooks@tamu.edu

PLATFORM: ATLANTIS

LOCATION: N/A

ASSOCIATED_DATA: See GPS info above

INSTRUMENT_INFO: Cloud Condensation Nuclei Counter (DMT CCN).

DATA_INFO: The data is reported as the mean concentration of aerosol particles in #/ccm in the time window between startUTC and stopUTC, but not including the times when particles had not yet traveled through the DMA column to the instruments.

UNCERTAINTY: Uncertainties in the optical particle counter (OPC) for the CCN of +/- 10% for one standard deviation is based on uncertainties in OPC temperature, volumetric flow rate, particle coincidence rate both in physical space and the data acquisition electronics, and the absolute pressure at the inlet. The standard deviation in supersaturation is reported in the data. The supersaturation uncertainty is estimated conservatively at +/- 0.03%, where variation in the inlet temperature, pressure, and calibration technique prevent a more accurate measurement.

ULOD_FLAG: -7777

ULOD_VALUE: N/A

LLOD_FLAG: -8888

LLOD_VALUE: N/A

DM_CONTACT_INFO: See PI

PROJECT_INFO: NAAMES 2018 Mission

STIPULATIONS_ON_USE: N/A

OTHER_COMMENTS: N/A

REVISION: R0

startUTC,stopUTC,ss,nccn,lat,lon,alt

dNdlogDp_12120pm, #/cc
dNdlogDp_12920pm, #/cc
dNdlogDp_13770pm, #/cc
dNdlogDp_14690pm, #/cc
dNdlogDp_15660pm, #/cc
dNdlogDp_16710pm, #/cc
dNdlogDp_17820pm, #/cc
dNdlogDp_19010pm, #/cc
dNdlogDp_20280pm, #/cc
dNdlogDp_21640pm, #/cc
dNdlogDp_23100pm, #/cc
dNdlogDp_24650pm, #/cc
dNdlogDp_26320pm, #/cc
dNdlogDp_28100pm, #/cc
dNdlogDp_30010pm, #/cc
dNdlogDp_32050pm, #/cc
dNdlogDp_34240pm, #/cc
dNdlogDp_36590pm, #/cc
dNdlogDp_39100pm, #/cc
dNdlogDp_41810pm, #/cc
dNdlogDp_44710pm, #/cc
dNdlogDp_47800pm, #/cc
dNdlogDp_51180pm, #/cc

dNdlogDp_54790pm, #/cc
dNdlogDp_58680pm, #/cc
dNdlogDp_62870pm, #/cc
dNdlogDp_67390pm, #/cc
dNdlogDp_72280pm, #/cc
dNdlogDp_77560pm, #/cc
dNdlogDp_83270pm, #/cc
dNdlogDp_89470pm, #/cc
dNdlogDp_96200pm, #/cc
dNdlogDp_103510pm, #/cc
dNdlogDp_111470pm, #/cc
dNdlogDp_120150pm, #/cc
dNdlogDp_129630pm, #/cc
dNdlogDp_140000pm, #/cc
dNdlogDp_151380pm, #/cc
dNdlogDp_163880pm, #/cc
dNdlogDp_177640pm, #/cc
dNdlogDp_192810pm, #/cc
dNdlogDp_209590pm, #/cc
dNdlogDp_228090pm, #/cc
dNdlogDp_248800pm, #/cc
dNdlogDp_271750pm, #/cc
dNdlogDp_297320pm, #/cc

dNdlogDp_325870pm, #/cc

dNdlogDp_357800pm, #/cc

dNdlogDp_393560pm, #/cc

dNdlogDp_433660pm, #/cc

dNdlogDp_478690pm, #/cc

dNdlogDp_529310pm, #/cc

dNdlogDp_586260pm, #/cc

dNdlogDp_650390pm, #/cc

dNdlogDp_722650pm, #/cc

dNdlogDp_804150pm, #/cc

dNdlogDp_896130pm, #/cc

SEMS_Total_Conc, #/cc

1

dNdlogDp_{diameter in picometer (pm)}

18

PI_CONTACT_INFO: 858-534-4852; 9500 Gilman Drive, La jolla, CA 92093-0221;

lmrussell@ucsd.edu

PLATFORM: R/V Atlantis

LOCATION: North Atlantic

ASSOCIATED_DATA: N/A

INSTRUMENT_INFO: Scanning Electrical Mobility Sizer (SEMS), Model 2002

DATA_INFO: Aerosol Number distribution in dN/dlogDp (number_per_cubiccentimeter) at ambient temperature and pressure

UNCERTAINTY: Please contact the PI for uncertainty information

ULOD_FLAG: -7777

ULOD_VALUE: N/A

LLOD_FLAG: -8888

LLOD_VALUE: N/A

DM_CONTACT_INFO: Data Manager: Raghu Betha; Scripps Institution of Oceanography;
858-534-6856; 8861 Shellback way, Rm 229, La Jolla, CA 92093; rbetha@ucsd.edu

PROJECT_INFO: NAAMES3 study; 08/30/2017 - 09/24/2017; <http://naames.larc.nasa.gov/>

STIPULATIONS_ON_USE: Use of these data require prior ok from PI.

OTHER_COMMENTS:

REVISION: RA

R0: Preliminary Data. For in-field use only.

Start_Time_UTC, Stop_Time_UTC, dNdlogDp_10000pm, dNdlogDp_10660pm,
dNdlogDp_11360pm, dNdlogDp_12120pm, dNdlogDp_12920pm, dNdlogDp_13770pm,
dNdlogDp_14690pm, dNdlogDp_15660pm, dNdlogDp_16710pm, dNdlogDp_17820pm,
dNdlogDp_19010pm, dNdlogDp_20280pm, dNdlogDp_21640pm, dNdlogDp_23100pm,
dNdlogDp_24650pm, dNdlogDp_26320pm, dNdlogDp_28100pm, dNdlogDp_30010pm,
dNdlogDp_32050pm, dNdlogDp_34240pm, dNdlogDp_36590pm, dNdlogDp_39100pm,
dNdlogDp_41810pm, dNdlogDp_44710pm, dNdlogDp_47800pm, dNdlogDp_51180pm,
dNdlogDp_54790pm, dNdlogDp_58680pm, dNdlogDp_62870pm, dNdlogDp_67390pm,
dNdlogDp_72280pm, dNdlogDp_77560pm, dNdlogDp_83270pm, dNdlogDp_89470pm,
dNdlogDp_96200pm, dNdlogDp_103510pm, dNdlogDp_111470pm, dNdlogDp_120150pm,
dNdlogDp_129630pm, dNdlogDp_140000pm, dNdlogDp_151380pm, dNdlogDp_163880pm,

dNdlogDp_177640pm, dNdlogDp_192810pm, dNdlogDp_209590pm, dNdlogDp_228090pm,
dNdlogDp_248800pm, dNdlogDp_271750pm, dNdlogDp_297320pm, dNdlogDp_325870pm,
dNdlogDp_357800pm, dNdlogDp_393560pm, dNdlogDp_433660pm, dNdlogDp_478690pm,
dNdlogDp_529310pm, dNdlogDp_586260pm, dNdlogDp_650390pm, dNdlogDp_722650pm,
dNdlogDp_804150pm, dNdlogDp_896130pm, SEMS_Total_Conc

dNdlogDp_12120pm, #/cc
dNdlogDp_12920pm, #/cc
dNdlogDp_13770pm, #/cc
dNdlogDp_14690pm, #/cc
dNdlogDp_15660pm, #/cc
dNdlogDp_16710pm, #/cc
dNdlogDp_17820pm, #/cc
dNdlogDp_19010pm, #/cc
dNdlogDp_20280pm, #/cc
dNdlogDp_21640pm, #/cc
dNdlogDp_23100pm, #/cc
dNdlogDp_24650pm, #/cc
dNdlogDp_26320pm, #/cc
dNdlogDp_28100pm, #/cc
dNdlogDp_30010pm, #/cc
dNdlogDp_32050pm, #/cc
dNdlogDp_34240pm, #/cc
dNdlogDp_36590pm, #/cc
dNdlogDp_39100pm, #/cc
dNdlogDp_41810pm, #/cc
dNdlogDp_44710pm, #/cc
dNdlogDp_47800pm, #/cc
dNdlogDp_51180pm, #/cc

dNdlogDp_54790pm, #/cc
dNdlogDp_58680pm, #/cc
dNdlogDp_62870pm, #/cc
dNdlogDp_67390pm, #/cc
dNdlogDp_72280pm, #/cc
dNdlogDp_77560pm, #/cc
dNdlogDp_83270pm, #/cc
dNdlogDp_89470pm, #/cc
dNdlogDp_96200pm, #/cc
dNdlogDp_103510pm, #/cc
dNdlogDp_111470pm, #/cc
dNdlogDp_120150pm, #/cc
dNdlogDp_129630pm, #/cc
dNdlogDp_140000pm, #/cc
dNdlogDp_151380pm, #/cc
dNdlogDp_163880pm, #/cc
dNdlogDp_177640pm, #/cc
dNdlogDp_192810pm, #/cc
dNdlogDp_209590pm, #/cc
dNdlogDp_228090pm, #/cc
dNdlogDp_248800pm, #/cc
dNdlogDp_271750pm, #/cc
dNdlogDp_297320pm, #/cc

dNdlogDp_325870pm, #/cc

dNdlogDp_357800pm, #/cc

dNdlogDp_393560pm, #/cc

dNdlogDp_433660pm, #/cc

dNdlogDp_478690pm, #/cc

dNdlogDp_529310pm, #/cc

dNdlogDp_586260pm, #/cc

dNdlogDp_650390pm, #/cc

dNdlogDp_722650pm, #/cc

dNdlogDp_804150pm, #/cc

dNdlogDp_896130pm, #/cc

SEMS_Total_Conc, #/cc

1

dNdlogDp_{diameter in picometer (pm)}

18

PI_CONTACT_INFO: 858-534-4852; 9500 Gilman Drive, La jolla, CA 92093-0221;

lmrussell@ucsd.edu

PLATFORM: R/V Atlantis

LOCATION: North Atlantic

ASSOCIATED_DATA: N/A

INSTRUMENT_INFO: Scanning Electrical Mobility Sizer (SEMS), Model 2002

DATA_INFO: Aerosol Number distribution in dN/dlogDp (number_per_cubiccentimeter) at ambient temperature and pressure

UNCERTAINTY: Please contact the PI for uncertainty information

ULOD_FLAG: -7777

ULOD_VALUE: N/A

LLOD_FLAG: -8888

LLOD_VALUE: N/A

DM_CONTACT_INFO: Data Manager: Georges Saliba; Scripps Institution of Oceanography;
412-908-1321; 8861 Shellback way, Rm 229, La Jolla, CA 92093; gesaliba@ucsd.edu

PROJECT_INFO: NAAMES4 study; 03/20/2018 - 04/13/2018; <http://naames.larc.nasa.gov/>

STIPULATIONS_ON_USE: Use of these data require prior ok from PI.

OTHER_COMMENTS:

REVISION: R0

R0: Preliminary Data. For in-field use only.

Start_Time_UTC, Stop_Time_UTC, dNdlogDp_10000pm, dNdlogDp_10660pm,
dNdlogDp_11360pm, dNdlogDp_12120pm, dNdlogDp_12920pm, dNdlogDp_13770pm,
dNdlogDp_14690pm, dNdlogDp_15660pm, dNdlogDp_16710pm, dNdlogDp_17820pm,
dNdlogDp_19010pm, dNdlogDp_20280pm, dNdlogDp_21640pm, dNdlogDp_23100pm,
dNdlogDp_24650pm, dNdlogDp_26320pm, dNdlogDp_28100pm, dNdlogDp_30010pm,
dNdlogDp_32050pm, dNdlogDp_34240pm, dNdlogDp_36590pm, dNdlogDp_39100pm,
dNdlogDp_41810pm, dNdlogDp_44710pm, dNdlogDp_47800pm, dNdlogDp_51180pm,
dNdlogDp_54790pm, dNdlogDp_58680pm, dNdlogDp_62870pm, dNdlogDp_67390pm,
dNdlogDp_72280pm, dNdlogDp_77560pm, dNdlogDp_83270pm, dNdlogDp_89470pm,
dNdlogDp_96200pm, dNdlogDp_103510pm, dNdlogDp_111470pm, dNdlogDp_120150pm,
dNdlogDp_129630pm, dNdlogDp_140000pm, dNdlogDp_151380pm, dNdlogDp_163880pm,

dNdlogDp_177640pm, dNdlogDp_192810pm, dNdlogDp_209590pm, dNdlogDp_228090pm,
dNdlogDp_248800pm, dNdlogDp_271750pm, dNdlogDp_297320pm, dNdlogDp_325870pm,
dNdlogDp_357800pm, dNdlogDp_393560pm, dNdlogDp_433660pm, dNdlogDp_478690pm,
dNdlogDp_529310pm, dNdlogDp_586260pm, dNdlogDp_650390pm, dNdlogDp_722650pm,
dNdlogDp_804150pm, dNdlogDp_896130pm, SEMS_Total_Conc